2006-12

Ocean mixed layer response to gap wind scenarios

Konstantinou, Nikolaos

Monterey, California. Naval Postgraduate School

NAVAL POSTGRADUATE SCHOOL

MONTEREY, CALIFORNIA

THESIS

OCEAN MIXED LAYER RESPONSE TO GAP WIND SCENARIOS

by

Nikolaos Konstantinou

December 2006

Thesis Advisor:	Qing Wang
Co-Advisor:	Roland W. Garwood

Approved for public release; distribution is unlimited

THIS PAGE INTENTIONALLY LEFT BLANK

REPORT DOCUMENTATION PAGE	Form Approved OMB No. 0704-0188

1. AGENCY USE ONLY *(Leave blank)*	2. REPORT DATE December 2006	3. REPORT TYPE AND DATES COVERED Master's Thesis

4. TITLE AND SUBTITLE Ocean Mixed Layer Response to Gap Wind Scenarios	5. FUNDING NUMBERS
6. AUTHOR(S) Nikolaos Konstantinou	
7. PERFORMING ORGANIZATION NAME(S) AND ADDRESS(ES) Naval Postgraduate School Monterey, CA 93943-5000	8. PERFORMING ORGANIZATION REPORT NUMBER
9. SPONSORING /MONITORING AGENCY NAME(S) AND ADDRESS(ES) Hellenic Navy General Staff Athens, Greece	10. SPONSORING/MONITORING AGENCY REPORT NUMBER

11. SUPPLEMENTARY NOTES The views expressed in this thesis are those of the author and do not reflect the official policy or position of the Department of Defense or the U.S. Government.

12a. DISTRIBUTION / AVAILABILITY STATEMENT **Approved for public release; distribution is unlimited**	12b. DISTRIBUTION CODE

13. ABSTRACT (maximum 200 words)

This study focuses on understanding the oceanic response to gap outflow and the air-sea interaction processes during the gap wind event between 26 and 28, February 2004 over the Gulf of Tehuantepec, Mexico. The U.S. Navy's Coupled Ocean Atmospheric Mesoscale Prediction System (COAMPS) and NPS Ocean Mixed Layer (OML) model was used to simulate the gap wind event and the temporal/spatial evolution of ocean response. Satellites, coincident in situ aircraft and AXBTs measurements of the sea surface temperature and the water temperature profiles collected during the Gulf of Tehuantepec Experiment (GOTEX) were used to define model initial conditions and aid the analysis of model results.

Results from the OML simulations suggest measurable SST evolution as a result of the enhanced upper ocean mixing along the jet axes. Model sensitivity tests show the dominant effects of surface heat flux in generating upper ocean mixing while mechanical forcing by the strong wind of the gap outflow has secondary effects. Sensitivity tests also suggest that the thermocline structure is the most important factor in determining the magnitude of the ocean response while variations in SST are not sensitive to upwelling for a short time scale of several days. The study of COAMPS/OML simulations and satellite (SST) images confirm the existence of a secondary gap outflow source in the area.

14. SUBJECT TERMS Ocean mixed layer, Gap winds, Sea surface temperature, Air-sea interaction.	15. NUMBER OF PAGES 81
	16. PRICE CODE

17. SECURITY CLASSIFICATION OF REPORT	18. SECURITY CLASSIFICATION OF THIS PAGE	19. SECURITY CLASSIFICATION OF ABSTRACT	20. LIMITATION OF ABSTRACT
Unclassified	Unclassified	Unclassified	UL

NSN 7540-01-280-5500 Standard Form 298 (Rev. 2-89)
Prescribed by ANSI Std. 239-18

THIS PAGE INTENTIONALLY LEFT BLANK

Approved for public release; distribution is unlimited

OCEAN MIXED LAYER RESPONSE TO GAP WIND SCENARIOS

Nikolaos Konstantinou
Lieutenant, Hellenic Navy
B.S., Hellenic Naval Academy, 1992

Submitted in partial fulfillment of the
requirements for the degree of

MASTER OF SCIENCE IN METEOROLOGY

from the

NAVAL POSTGRADUATE SCHOOL
December 2006

Author: Nikolaos Konstantinou

Approved by: Qing Wang
Thesis Advisor

Roland W. Garwood
Co-Advisor

Philip A. Durkee
Chairman, Department of Meteorology

THIS PAGE INTENTIONALLY LEFT BLANK

ABSTRACT

This study focuses on understanding the oceanic response to gap outflow and the air-sea interaction processes during the gap wind event between 26 and 28, February 2004 over the Gulf of Tehuantepec, Mexico. The U.S. Navy's Coupled Ocean Atmospheric Mesoscale Prediction System (COAMPS) and NPS Ocean Mixed Layer (OML) model was used to simulate the gap wind event and the temporal/spatial evolution of ocean response. Satellites, coincident in situ aircraft and AXBTs measurements of the sea surface temperature and the water temperature profiles collected during the Gulf of Tehuantepec Experiment (GOTEX) were used to define model initial conditions and aid the analysis of model results.

Results from the OML simulations suggest measurable SST evolution as a result of the enhanced upper ocean mixing along the jet axes. Model sensitivity tests show the dominant effects of surface heat flux in generating upper ocean mixing while mechanical forcing by the strong wind of the gap outflow has secondary effects. Sensitivity tests also suggest that the thermocline structure is the most important factor in determining the magnitude of the ocean response while variations in SST are not sensitive to upwelling for a short time scale of several days. The study of COAMPS/OML simulations and satellite (SST) images confirm the existence of a secondary gap outflow source in the area.

THIS PAGE INTENTIONALLY LEFT BLANK

TABLE OF CONTENTS

THIS PAGE INTENTIONALLY LEFT BLANK

LIST OF FIGURES

THIS PAGE INTENTIONALLY LEFT BLANK

LIST OF TABLES

THIS PAGE INTENTIONALLY LEFT BLANK

ACKNOWLEDGMENTS

I would like to thank the following people who have contributed significantly to the completion of this work:

- Dr. Shouping Wang, NRL/MRY for COAMPS simulations.
- Prof. Roland Garwood for knowledge and advice.
- Dr. K. Melville (Scripps) and Carl Friehe (U.C Irvine) for aircraft and AXBT measurements.
- Bob Creasy for help with Unix coding.
- CDR Rebecca Stones USN for information on oceanic data sources.
- Dr. John Kalogiros and Kostas Rados for helpful discussions and MATLAB codes.
- LT. Robin Corey Cherrett USN for advice and discussions.

Professor Qing Wang, thank you for your dedication, perspective and patience. I appreciate your effort, interest, and support. It was an unique experience working with you.

I would also like to thank the Hellenic Navy for providing the opportunity to pursue my studies at the Naval Postgraduate School.

Finally, I would like to dedicate this work to my wife and son, Georgiana and George, for their love, support, patience, and understanding during my studies at NPS.

THIS PAGE INTENTIONALLY LEFT BLANK

I. INTRODUCTION

The East Pacific warm pool (EPWP-Gulf of Tehuantepec (GoT)) is an ideal area for air-sea interaction study because of the frequent occurrence of strong gap wind during the winter seasons. Between November and February, when a low pressure system develops behind the lee side of Sierra Madre mountain ranges, cold surges penetrate into Central America and establish strong cross barrier pressure gradient in the Gulf of Tehuantepec region. Such pressure gradient resulted in strong gap wind across several gap or narrow passes in the region, one of which is the Chivela Pass. As the gap wind exits the Chivela pass, strong wind continues over the water that extends hundreds of kilometers into the Eastern Pacific. Maximum wind over the GoT can reach 60 knots (Stumpf, 1975). These high wind events are referred to as Tehuano. The high wind of the Tehuano creates regions of strong mixing and cooling of ocean waters that can lower the sea surface temperature (SST) as much as 8^{o}C in a few hours (e.g., Stumpf 1975). Consequently, the GoT region is a natural laboratory for studying the strong coupling between the atmosphere and the upper ocean.

The objective of this thesis is to understand the feedback process of air-sea interaction under strong atmospheric forcing using a one-dimensional ocean mixed layer model and atmospheric forcing from a high-resolution three-dimensional atmospheric mesoscale model. The ocean mixed layer model was originally described in Garwood (1977) and has been used in many previous studies of the oceanic response to various atmospheric scenarios (e.g.,

Elseberry 1980, Adamec 1984 and Chu 1990). The atmospheric mesoscale model is the atmospheric component of U.S.Navy's Coupled Ocean and Atmospheric Mesoscale Prediction System (COAMPS, Hodur 1997). There are already a lot of studies on the general dynamics and case analyses of the gap wind field and the interaction with the strong cross-mountain pressure gradients and the local topography for this area. Also there are studies using climatologically data for the air-sea coupling with very useful results about the upper ocean response to the strong winds. No research has been done in this region from a perspective of a strongly air-sea coupled system with high resolution in situ data. This is in part due to the lack of in situ observations in this area that makes model validation/evaluation difficult. The air-sea interaction in the area has been recognized as most important factors in determining the evolution of the upper ocean response. Although not a tightly coupled system, the combination of the OML model and COAMPS allow us to examine the ocean response to the Tehuano event with a clear understanding of multiple aspects of the coupling process and hence provide guidance for the development of a fully coupled system.

This research is also aided with the in situ measurements from the Gulf of Tehuantepec Experiment (GOTEX-February 2004) where extensive measurements of the atmospheric and the oceanic boundary layer during gap flow conditions were made by a research aircraft with dropsonde and AXBTs. This dataset gave us the unique opportunity to examine the results from the mesoscale model as well as from the 1-D mixed layer model.

Prediction of the evolution of the oceanic boundary layer is one of the primary concerns of geophysicist. It is also crucial to military operations as the performance of acoustic systems is affected by the conditions of the upper ocean. Many past studies have recognized a need of using the coupled prediction system as a tool to understand the atmosphere/ocean system particularly in conditions of strong atmospheric forcing and rapid oceanic response such as in a hurricane overpass. However, there are many unanswered questions about how the coupling occurs and how one should treat it in the modeling system. The OML model approach does not intend to replace the fully coupled three-dimensional time evolving forecast models currently under development elsewhere. However, this thesis research intends to answer some of the specific questions that will be helpful for the development of fully coupled 3-D ocean and atmospheric models.

THIS PAGE INTENTIONALLY LEFT BLANK

II. BACKGROUND

A. PHYSICAL PROCESSES IN THE OCEAN MIXED LAYER

The ocean mixed layer (OML) is the upper part of the ocean in which temperature and salinity are well mixed such that they are nearly constant with depth. The depth of the mixed layer usually ranges between 10-100 m. The thermocline is that part of the ocean that follows the mixed layer where the temperature is large.

The ocean mixed layer serves as a buffer zone between the atmospheric and deep oceanic circulations. The upper part of the thermocline changes with the season, so it is referred to as the seasonal thermocline. Below the seasonal thermocline, is the permanent thermocline where the temperature and salinity gradient remain nearly constant. The permanent thermocline to depths of 1500-2000 m. Figure 1 displays an example of the growth and decay of the mixed layer and seasonal thermocline (http://oceanworld.tamu.edu/resources/ocng textbook , last visited 26 October 2006).

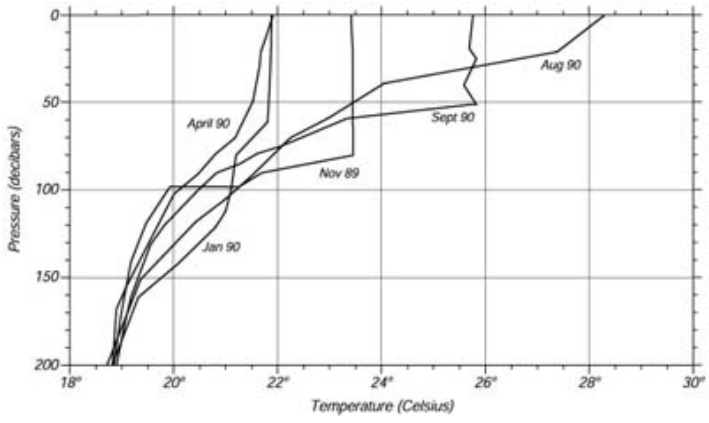

Figure 1. Growth and decay of the mixed layer and seasonal thermocline from November 1989 to September 1990 at the Bermuda Atlantic Time-series Station (BATS) (from http://oceanworld.tamu.edu/resources/ocng textbook /chapter6 last visited 26 October 2006).

Figure 1 shows the shallowing of the OML in the summer seasons and the deepening during the winter seasons. The evolution of the OML is controlled by several factors, including heat fluxes on the ocean surface, wind stress, precipitation/evaporation, net solar and infrared radiation. These processes are illustrated in Figure 2.

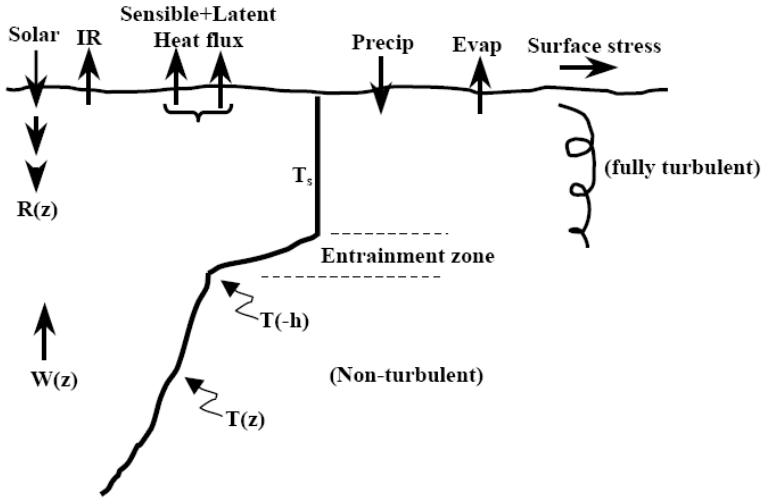

Figure 2. The processes that drive the temperature/depth of mixed layer (from Atmospheric-Ocean Dynamics, By Adrian E. Gill, 1982).

Wind blowing on the ocean mixes the upper layers leading to a thin mixed layer at the sea surface having approximately constant temperature and salinity from the surface down to a depth where the values differ from those at the surface. The depth and temperature of the mixed layer changes from day to day and from season to season in response to heat fluxes and turbulence. Heat fluxes through the surface heat and cool the surface waters. Variations in temperature change the density difference between the mixed layer and deeper waters. The greater the difference means that more work (energy) is needed to mix the layer downward and vice versa. Turbulence in the mixed layer mixes heat

downward. The turbulence depends on the intensity of breaking waves and the wind stress.

The turbulent mixing in the mixed layer is strongly affected by solar insolation. The differential absorption of the shortwave radiation results in warming of the water column and the strongest warming is generally found in the top layers of the water. Hence solar radiation stablizes the upper ocean, prevents turbulence mixing, and warms the upper layers. This mechanism explains the diurnal variation of the ocean mixed layers. It also explains the shallow mixed layer in the low latitudes compared to those in the Polar Regions (http://oceanworld.tamu.edu/resources/ocng textbook , last visited 26 October 2006).

B. GAP WINDS AND GAP FLOW

Gap winds are low level winds that are associated with flow going through gaps or low terrain. Gap winds under specific circumstances can have a magnitude of 50-60 Knots and the flow can extent for hundreds of miles (Clarke 1988, Cherrett 2006). The magnitude of these winds usually depends on the pressure gradient across the gap which is controlled by large scale synoptic conditions.

The maximum speed of the gap flow does not take place in the narrowest part of the gap as would be expected from a simple channel flow or the Bernoulli flow. Instead, the strongest wind occurs in the exit region of the gap. There are two reasons that can explain this. As the air flow approaches the gap, the depth of the air increases because of the blocking of terrain to the sides of the gap, which creates high pressure in the center and upwind of the gap. This pressure build-up slows down the air flow at the entrance (http://meted.ucar.edu/mesoprim/gapwinds/print.ht

ml, last visited 28 October 2006). In addition, in gap's exit region the air flow spreads out horizontally because of the widening of the gap. According to the conservation of mass this flow becomes thin, resulting in lower pressure in the exit region compared to the surroundings. Consequently, the pressure gradient along the gap increases and the wind along the gap accelerates.

Many gap outflows emerge over water (coastal regions), and often the maximum winds will be observed to occur over water downstream from the gap exit. (http://www.nrlmry.navy .mil/sat_training/dust/tokargap2/index.html, last visited 28 October 2006). This is due to the reduction of surface friction, instability introduced by cool air over relatively warmer water that promotes mixing of momentum to the surface from the higher winds aloft, and the existence of a pressure gradient near the exit of the gap (Mass et al., 1995).

In the coastal regions the gap outflow has a direct effect on sea surface temperature (SST) because of the enhanced mixing of the upper ocean. The oceanic response to the wind forcing includes the upwelling and entrainment of subsurface water into the surface layer, which can lower SST by as much as 8^{o}C in a few hours (Stumpf 1975; Stumpf and Legeckis 1977; Legeckis 1988; Trasvina et al. 1995; Schultz et al. 1997). Significant gap flows can be found all over the world, including the Gulf of Tehuantepec associated with the Chivela pass in central Mexico.

The affect of gap wind events on maritime and aviation military operations is very significant. The gap wind creates large wind shear that is one of the processes that create turbulent kinetic energy in the atmospheric boundary

layer (from http://apollo.lsc.vsc.edu/classes/met455 /notes /section4/1.html last visited 30 October 2006).

The Chivela Pass is the gap that cuts through the Sierra Madre of Mexico as displayed in Figure 3. The Sierra Madre mountain range separates the east Pacific Ocean from the Gulf of Mexico. The dimensions of the gap are 200 km long and 40 km wide and the maximum elevation of the gap is 250 m, while the barriers to the side of the gap reach the 2000 m to the west and 1500 m to the east. High winds are produced by this gap during the winter when there is high pressure gradient which is the result of a Central American cold surge (Reding 1992, Schultz et al. 1997).

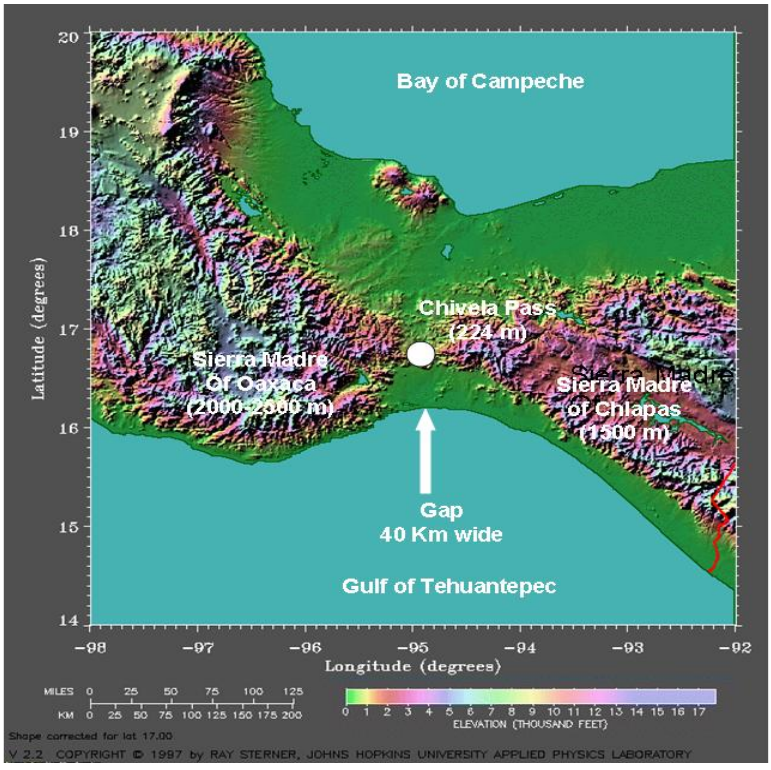

Figure 3. The Terrain map of the Chivela pass, Gulf of Tehuantepec, and surrounding area (from http://fermi.jhuapl.edu/states/ last visited 26 October 2006).

Many studies have been done on the atmospheric and oceanic characteristics of the GoT region associated with the gap wind. Those focusing on the atmospheric side of the GoT intended to understand the dynamical balance of the gap outflow region.

Several previous studies also focused on the oceanic response to the gap wind event in the GoT. The Chivela pass has very high influence on the surface waters. The strong outflow that is produced by the gap wind event results in substantial upper ocean mixing and produces an upwelling bringing cooler water to the surface.

The effect of the wind path on the SST of the Gulf was examined by Clarke (1988). Satellite measurements of sea surface temperature in combination with coastal wind data for the first 41 days of 1986 were examined for the influence on the SST for the Gulf of Tehuantepec. Daily satellite images suggest that the initial development of cold surface water in a clockwise loop is the result of the wind mixing the upper ocean layer.

Gap outflow wind enhances coastal upwelling. It is known that one of the processes that upwelling is depends on is the wind stress. Legeckis (1988) analyzed a gap flow event in the area from 7 to 22 March 1985.. He observed unusually persistent upwelling southwest of the Gulf of Panama and Gulf of Papagayo. During this period, the upwelling of the Gulf of Tehuantepec was relatively week compared to the Gulfs of Panama and Papagayo (south of the Gulf of Tehuantepec). It was postulated that the high pressure system was located farther south than usual and resulted in the maximum of the gap winds to be shifted from the Gulf of Tehuantepec to the other two Gulfs.

In a another case illustrating the ocean response and the influence on the thermocline depth was studied by Xie et al (2005), using high-resolution satellite observations, Xie et al., (2005), investigated air-sea interaction over the eastern Pacific warm pool. One of their conclusions was that the meridionally oriented Tehuantepec jets influence the local thermocline depth.

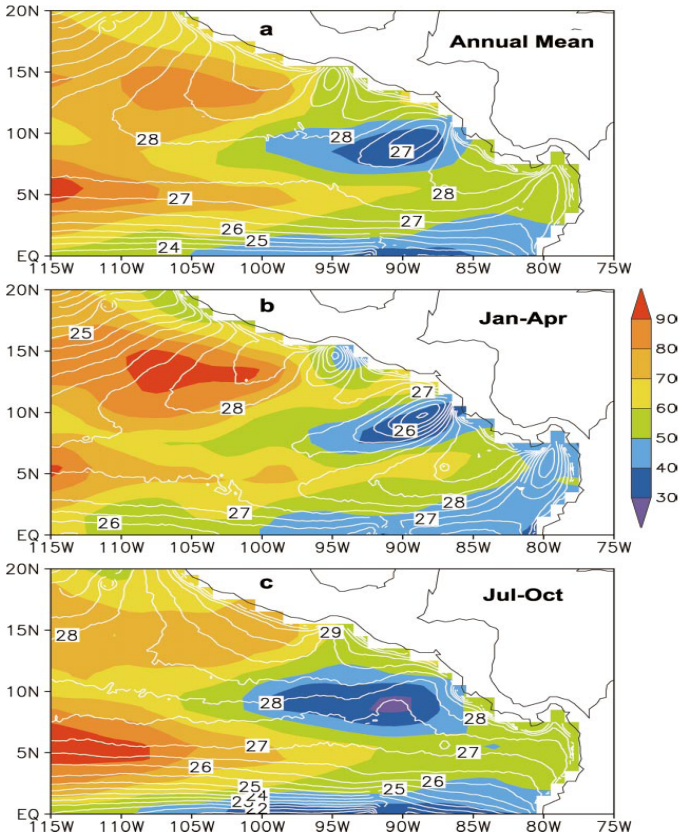

Figure 4. Climatology of SST (contours at intervals of 0.5°C) and the 20°C isotherm depth (color in (m)): (a) Annual mean, (b) Jan–Apr and (c) Jul–Oct. The patterns of SST during these two seasonal periods and the influence of the period (Jan.-Apr.) to the annual mean are displayed.

Sun and Yu (2006) studied the annual SST variations using the Regional Modeling System (ROMS) model. The annual mean SST was found to be strongly affected by wind jets

through gaps in the Central American mountains. Their results show that the local maxima of the amplitudes of the SST annual harmonics were caused by the gap winds (Fig. 5). The primary reason for this was the shallowing of the thermocline which allows cold water to be entrained in the upper ocean.

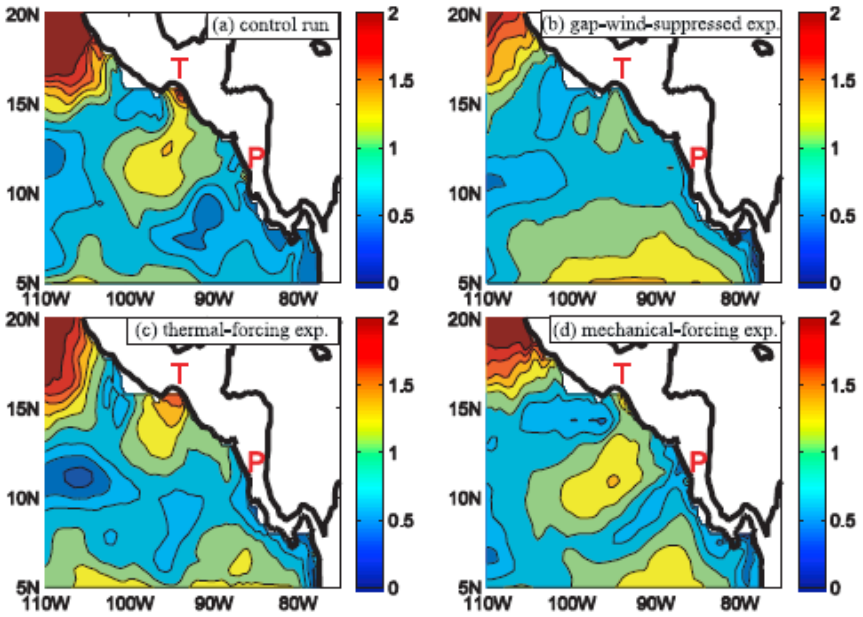

Figure 5. Amplitudes of SST annual harmonic (K) are displayed for four different experiments (from Sun and Yu 2006).

III MODELS AND DATA SOURCES

A. COUPLED OCEAN/ATMOSPHERE MESOSCALE PREDICTION SYSTEM (COAMPS™)

The U.S. Navy's coupled ocean/atmosphere mesoscale prediction system (COAMPS) is a three dimensional non hydrostatic mesoscale model. It implemented the most up-to-date physical parameterizations and utilizes an advanced data assimilation system. COAMPS has several options for high-resolution terrain data. This model can be used as a short-term forecast model (up to 72 hours) for any given region on earth. A detailed description of COAMPS numerical schemes, physical parameterizations and case studies can be found in Hodur (1997). The general theory and the equations can be found in Naval Research Laboratory (NRL) publication (COAMPS model description NRL/PU/7500--03-448 May 2003).

COAMPS is primarily running as an atmospheric mesoscale model, although the coupled capability is currently under development. COAMPS permits idealized or real-data case studies. In this case during COAMPS simulations the U.S. Navy's Operation Global Atmospheric Prediction System (NOGAPS) was used for the boundary conditions.

For this study, the grid resolution of the inner most domain is 3 Km. The inner domain covers the terrains of Central Mexico as well as the greater Gulf of Tehuantepec region. The COAMPS simulations were made by Naval Research Laboratory, Monterey, CA (Dr. S. Wang). The simulation started at 00Z 23 February, and ended at 12Z of 29 February 2004. Each forecast was made for a 72 hour period and a new run started every 12 hours.

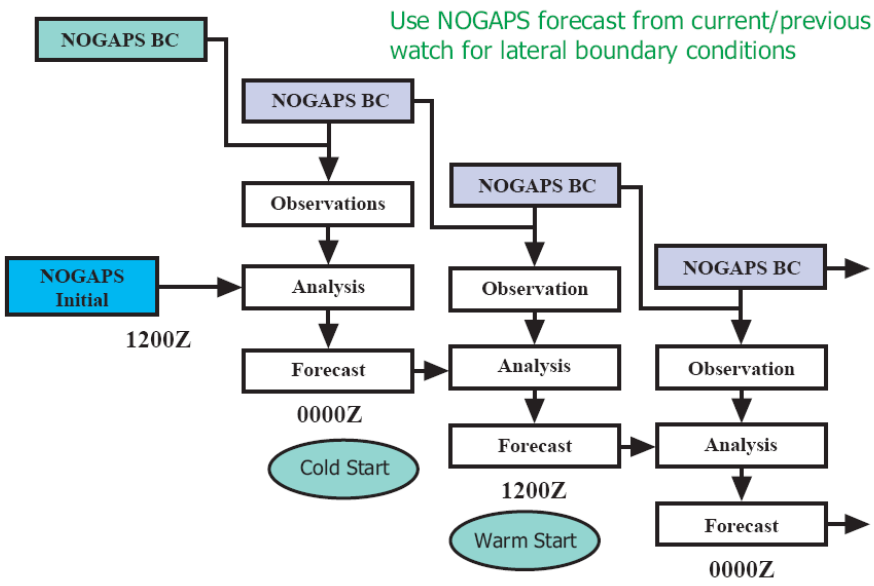

Figure 6. Schematic illustration of COAMPS data assimilation cycle (from NRL Publication NRL/PU/7500--03-448 May 2003.)

Code was developed for reading and plotting the results of COAMPS simulation. The atmospheric results of the simulation were also used for forcing the NPS ocean mixed layer model.

B. NPS OCEANIC MIXED LAYER MODEL

The ocean mixed layer model used in this thesis was developed by Prof. Roland W. Garwood at the Oceanography Department of the Naval Postgraduate School (Garwood 1977). We will here after refer to this model as the OML. The OML has been used in many previous studies of the oceanic response to various atmospheric scenarios (e.g., Elseberry 1980, Adamec 1984 and Chu 1990).

The OML is a one dimensional model of the mixed layer of the upper ocean. The model predicts mixed layer temperature, mixed layer depth, and ocean current using external forcing of surface momentum flux, sensible heat

flux, latent heat flux, net infrared and solar radiation. Initial conditions and upwelling are externally specified to the model.

In this model the entrainment depends on the relative distribution of horizontal and vertical components of turbulent kinetic energy. The portion of wind-generated turbulent kinetic energy is dependent upon two factors, the layer stability and the viscous dissipation which is enhanced for increased values of $Ro^{-1}=h f / u_*$, where f is the Coriolis parameter, h is mixed layer depth, and u_* the friction velocity for the water (Garwood 1977). The energy budget of the ocean mixed layer is displayed in Figure 7.

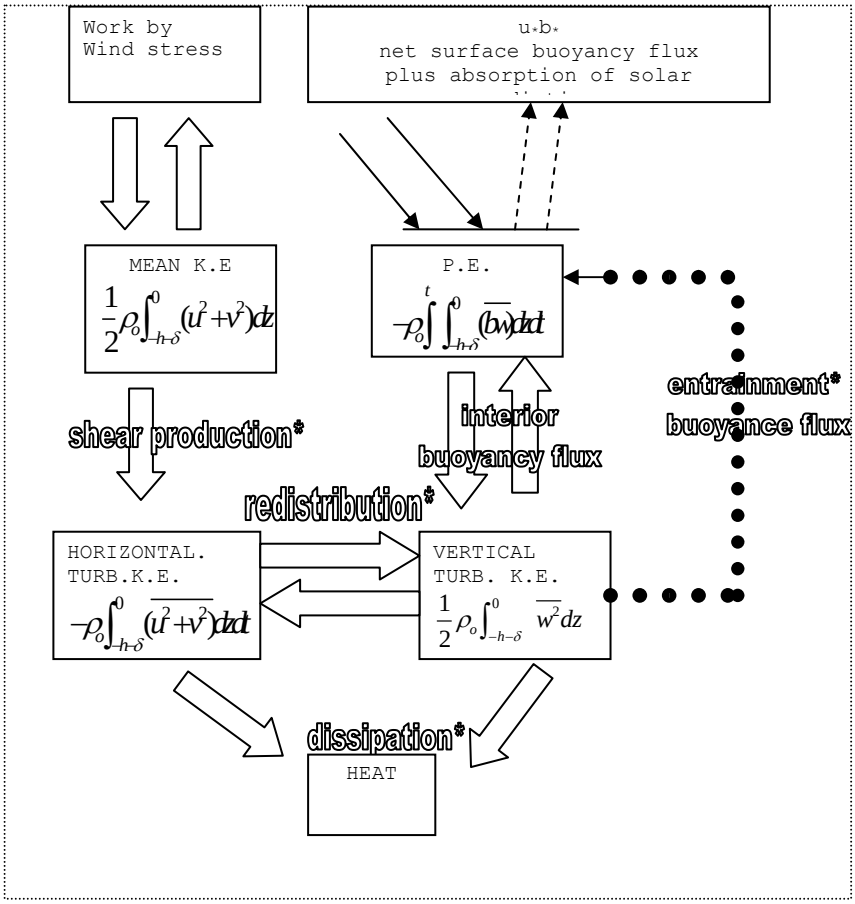

Figure 7. Mechanical energy budget for the ocean mixed layer. Asterisks indicate those processes that must be parameterized to close the system equations (from Garwood, 1977).

C. GULF OF TEHUANTEPEC EXPERIMENT (GOTEX)

The Gulf of Tehuantepec Experiment (GOTEX) took place from 1 February to 1 March 2004 over the Gulf of Tehuantepec. A research aircraft, the C-130Q Hercules operated by the National Center for Atmospheric Research (NCAR)/Research Aviation Facility (RAF), was the main measurement platform with 11 flights during the one month period. The objective of the GOTEX was to study the role of surface waves in coupling the marine boundary layer (MBL) and the marine atmospheric boundary layer (MABL) in moderate to high wind conditions. The GoT was selected because of the frequent occurrence of the gap wind events that take place during the winter season.

In addition to the standard C-130 instrument package, dropsondes and AXBTs were used to profile the marine atmospheric boundary layer (MABL) and the marine boundary layer (MBL). The measurements of the NCAR C-130 were used in this study to reveal and to identify uncertainties in sea surface temperature (SST). Also they were used for the evaluation of COAMPS/OML simulations. Details about the instrumentation and data variables can be found on http://www.eol.ucar.edu/raf/instruments.html (last visited 26 October 2006).

IV. MESOSCALE FORCING AND THE OBSERVED OCEAN RESPONSE

This chapter will focus on the development of the gap wind event that occurred between February 26 and 27, 2004 in the Gulf of Tehuantepec. This event will be referred to as GAP022604. The same event was studied by Cherrett (2006) with the emphases on the atmospheric boundary layer and surface characteristics of the gap outflow region. Since our focus here is on the upper ocean response to the gap outflow, the discussion starts before the onset of the gap event in order to understand the atmospheric forcing to the upper ocean and the initial upper ocean condition before the gap event. Here, we will briefly introduce the synoptic surface conditions that generated this event, examine the sea surface temperature variation observed from satellite, the NCAR C-130, and the upper ocean thermodynamic structure measured by the AXBTs released from the C-130. Further details of the synoptic analysis are given by Cherrett (2006).

A. SYNOPTIC CONDITIONS

The event of interest to this study (GAP022604) initiated from a strong surge of cold air along the eastern slopes of the Sierra Madre that created a strong gap outflow emerged from the Chivela Pass. This scenario depicts a typical synoptic condition that results in gap events as described in Steenburgh *et al.* (1998). Here, this synoptic forcing will be briefly discussed using the forecast from the Naval Operational Global Atmospheric Prediction System (NOGAPS).

Figures 8 and 9 show the surface pressure and the 925 mb geopotential heights from the NOGAPS forecast. At 00Z 24 February, a high pressure center of 1026 mb was located over north-east U.S. (not shown). A low pressure center of 1006 mb was located along the Texas and Mexico eastern coastline. A strong surge of cold air moved equatorward along the Sierra Madre (east side) into Mexico and Central America.

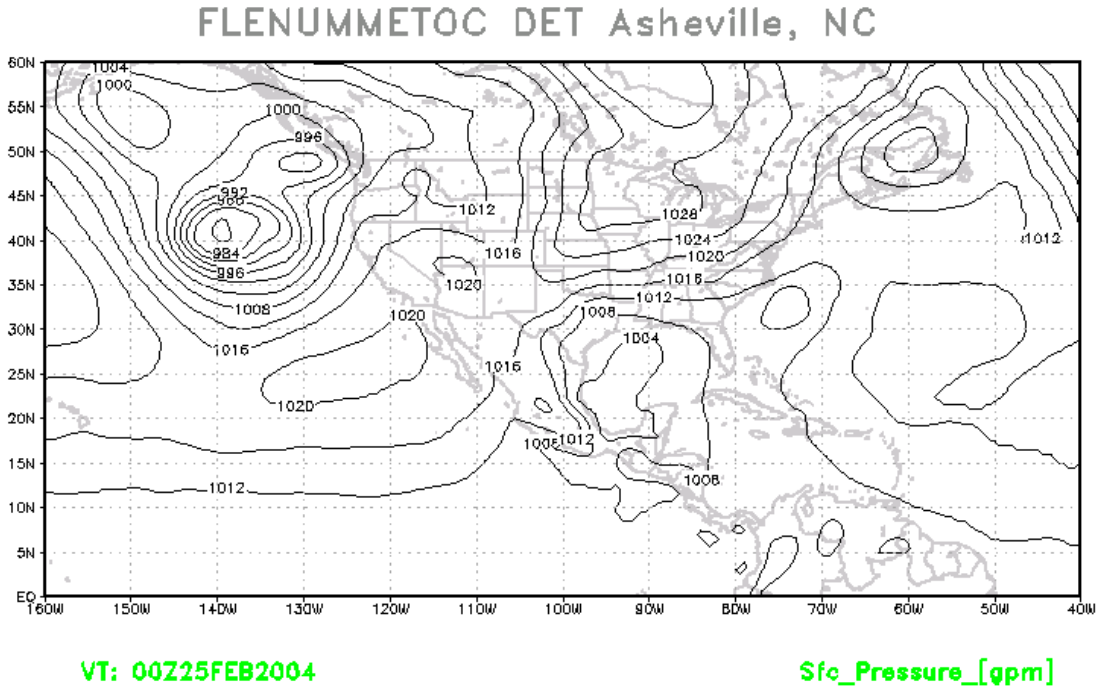

Figure 8. The NOGAPS analysis of surface pressure at 00Z 25 February 2004.

The surface pressure field at 00Z 25 February reveals the atmospheric conditions before the development of the gap outflow over the Gulf of Tehuantepec (Figure 8). At this time, the low pressure center had moved off the coast into the Gulf of Mexico and with a pressure of 1002 mb. The attendant cold front, denoting the leading edge of the cold surge, extended into south Mexico north of Chivela Pass.

The high pressure center over Minnesota had increased to 1030 mb and was moving southwest. This high pressure along the mountains was behind the cold front that had reached the southern area of Texas.

At 00Z 26 February the Tehuano event had already moved to the Pacific water through the Chivela pass. By 12Z of the same day, the cold front progressed south. The high pressure over the central U.S. extended down the eastern Mexican coast and a 6 mb pressure gradient across Chivela pass is created (Figure 9b).

(a)

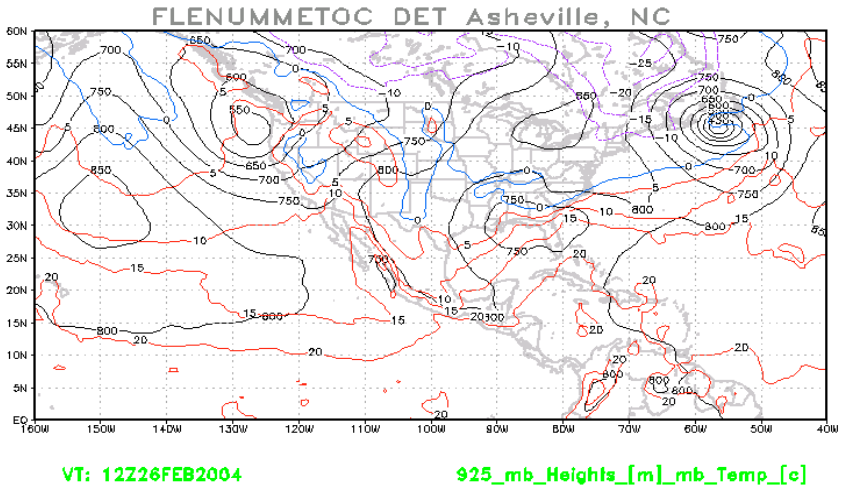

(b)

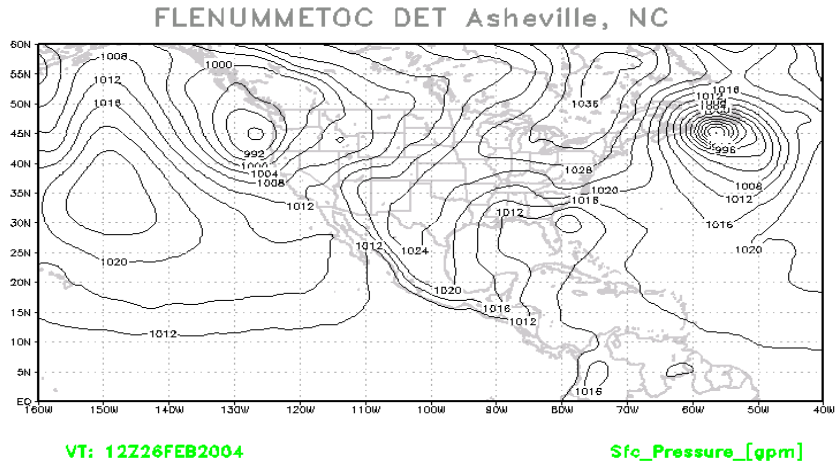

Figure 9. NOGAPS forecast for North America at 12Z February 26, 2004 (a) 925 mb heights and temperatures and (b) surface pressure.

The visible satellite imagery (GOES-12 band1) clearly shows the progression of the gap outflow in GAP022604 (Figure. 10). Because of the strong convergence at the gap outflow front, the leading edge of the gap outflow is characterized by the presence of "rope cloud" as discussed in Steenburg et al. (1998) and Cherrett (2006). Cherrett (2006) used the time variation of the location of the rope cloud and determined that the south-west ward progression of the outflow front moved at a speed of 30 km hr^{-1}. These isochrones can be used also as references to evaluate the performance of COAMPS atmospheric simulation for the event.

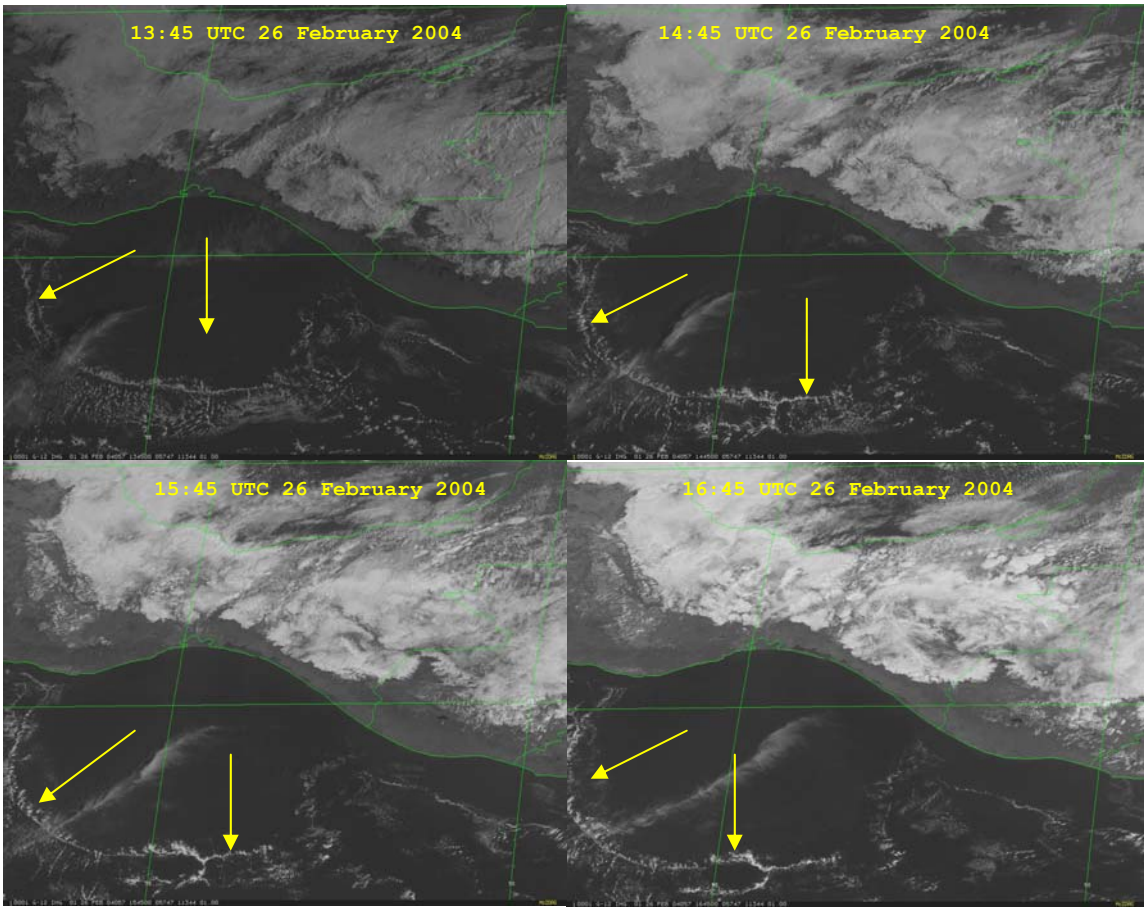

Figure 10. Isochrones of the leading edge (rope cloud indicated with yellow arrows).

B. COAMPS SIMULATION.

1. COAMPS Model Setup and Initialization.

COAMPS simulations were made by Dr. Shouping Wang at the Naval Research Laboratory at Monterey CA. The model setup was similar to Cherrett (2006) with a few exceptions. The COAMPS simulation for this thesis used a newer version of COAMPS which should not result in significant differences between the current results and those shown in Cherrett (2006). In addition to output variables discussed in Cherrett (2006), the new COAMPS run for this thesis research also included solar and longwave irradiance as atmospheric forcing of the ocean models. The COAMPS simulation for GAP022604 was initiated at 00Z 23 February 2004 and continued up to 12Z 29 February 2004. Every 12 hours the model was updated with new NOGAPS boundary conditions and data assimilation. Although each forecast of the COAMPS run continues for 72 hours, we only use the forecast between 12 and 24 hours after the start of each simulation. This selection of the forecast is considered optimal considering both the effect of initial conditions and decreasing forecast quality for longer periods of forecast. For analysis presented in this chapter, we will present results from 12Z 25 February, approximately 12 hours before the onset of the gap outflow.

2. COAMPS Predicted Development of Gap Outflow

a. Wind Field

Figure 11 shows the development of the gap outflow wind field in 3-hour intervals starting from 06Z of February 26, 2004. The COAMPS 10 m wind speed is contoured and color filled, and the wind direction and magnitude are also shown in the arrows on every fourth grid point. Figure 11a shows that the event had already begun at 06Z while the

remaining five panels show the development of the event. The distance of the outflow that reaches hundreds of kilometers offshore can be seen in the last four images. The highest winds peak at a magnitude of 22 m s^{-1} and occurred just offshore downstream of the gap. This offshore maximum was also noted by Steenburgh et al. (1998) and is in agreement with the gap flow theory as discussed in Chapter II.

The COAMPS wind field shows the existence of another smaller outflow to the south east side of the main gap outflow. This less extensive outflow is likely caused by the rising terrain east of Chivela Pass that forms a smaller pass to the west (the Chiapas). Unfortunately, the aircraft did not fly through this secondary outflow and the scatterometry can not measure the near coastal winds due to coastal contamination. However, as seen later in this chapter, the presence of the small gap outflow to the east of the main outflow is confirmed from satellite the measured SST field.

The presence of a second and weaker gap outflow in the GoT region was not predicted by MM5 in Steenburgh's research. This difference is mainly due to the difference in terrain resolution and model grid resolution. According to the results of the simulations between the two major jets an axis of relative minimum winds persists.

Although the gap flow near the center of jet appears to follow an inertial path, the surrounding flow does not necessarily follow such a path. The flow to the west of the core outflow jet experienced stronger anticyclonic curvature, while the flow to the east followed paths that were straight or curved cyclonically.

Comparing the observed leading edge from satellite images with COAMPS results indicates that COAMPS simulations did not match the progression in the southward and southeastward part of the outflow. The maximum wind jet core appears almost two degrees north compared to that seen from the scatterometer winds at the same longitude. Nevertheless, the western progression of the leading edge, and the wind speeds matched the outflow of the satellite imagery and the aircraft measured wind.

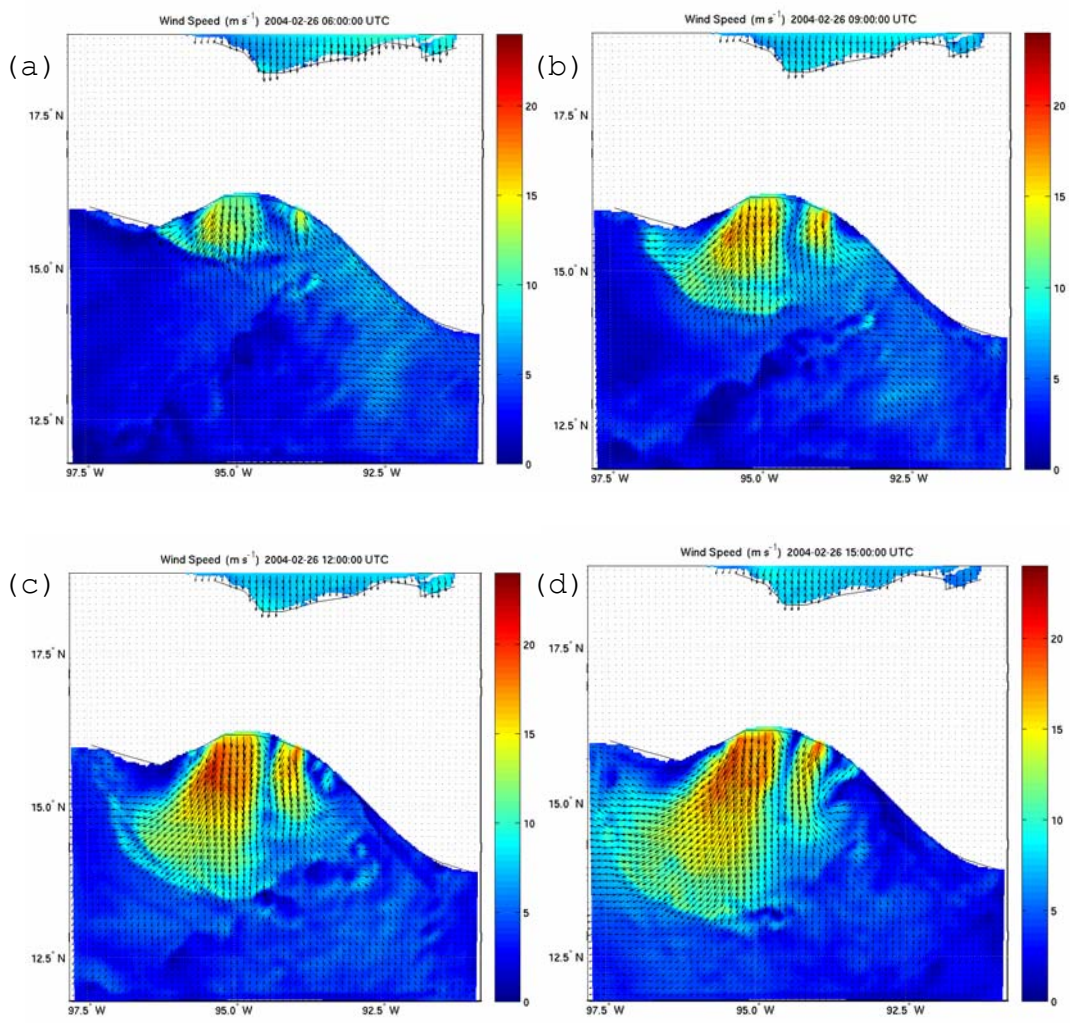

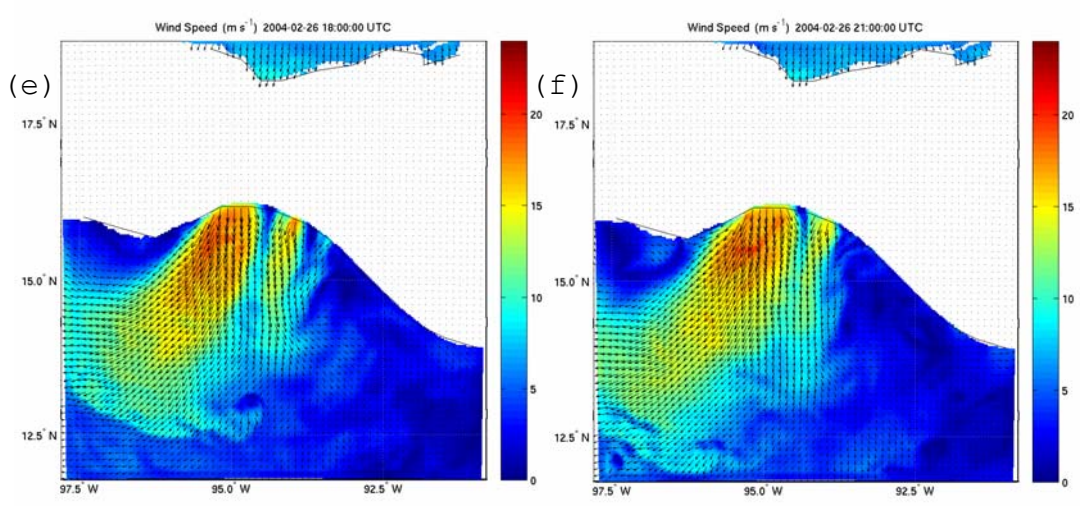

Figure 11. COAMPS simulated wind speed contours (in ms^{-1}) and wind vectors at 10 m analyzed on 26 February at (a) 06Z, (b) 09Z, (c) 12Z, (d) 15Z, (e) 18Z and (f) 21Z. The length of the wind vector is proportional to its magnitude

b. Wind Stress

Figure 12 shows the time evolution of the wind stress along with vectors showing the direction of COAMPS stress field. These panels are very similar to the wind speed variation in Figure 11. The wind field discussed earlier and all features discussed before apply here also for the wind stress field.

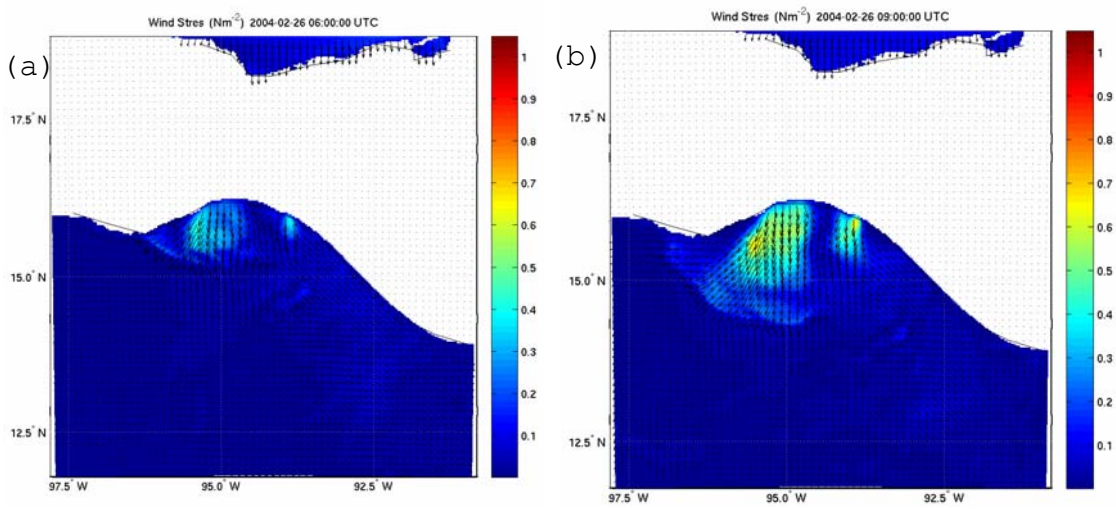

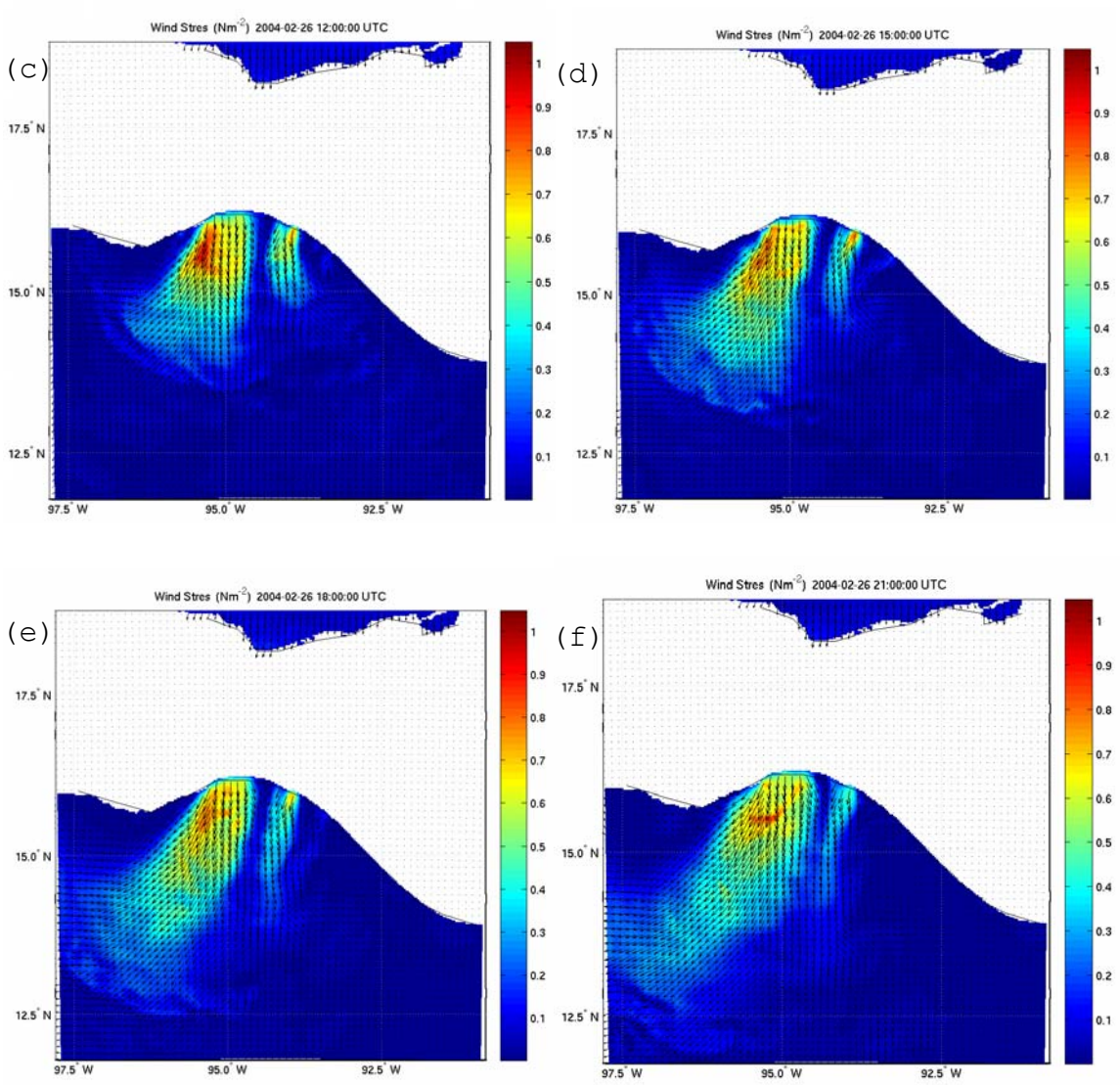

Figure 12. COAMPS simulated wind stress contours (in Nm^{-2}) and wind vectors at 10 m analyzed on 26 February at (a) 06Z, (b) 09Z, (c) 12Z, (d) 15Z, (e) 18z and (f) 21z. The length of the wind vector is proportional to its magnitude.

c. Surface Fluxes

Figure 13 shows the sensible heat flux at 3 hour intervals along with wind vectors of the COAMPS 10 m wind field. Sensible heat flux experiences strong diurnal variation although the diurnal variation is not readily seen here since all the panels are from the same day. Here we find the enhanced sensible heat flux behind the outflow

front with the maximum at the mouth of the GoT. The sensible heat flux can reach to a maximum of 160 Wm^{-2}.

Similar to air temperature (not shown), sensible heat flux shows strong diurnal variation. During the day when the daytime heating warms the ground temperature, the air flowing over the sea iss warm, resulting in smaller sensible heat flux. In Figures 13a, weak (but positive) sensible heat flux behind the outflow front was found as the gap wind reaches the mouth of GoT. As the jet wind speed developed, sensible heat flux increased considerably as time progressed and reached a maximum at around 15Z 26 February 2004 (07:00 LST). After sunrise (Figure 13e, 18Z, 26 February 2004 (10:00 LST)), the sensible heat flux field was weaker and become even weaker at noon (Figure 13f, 1300 LST).

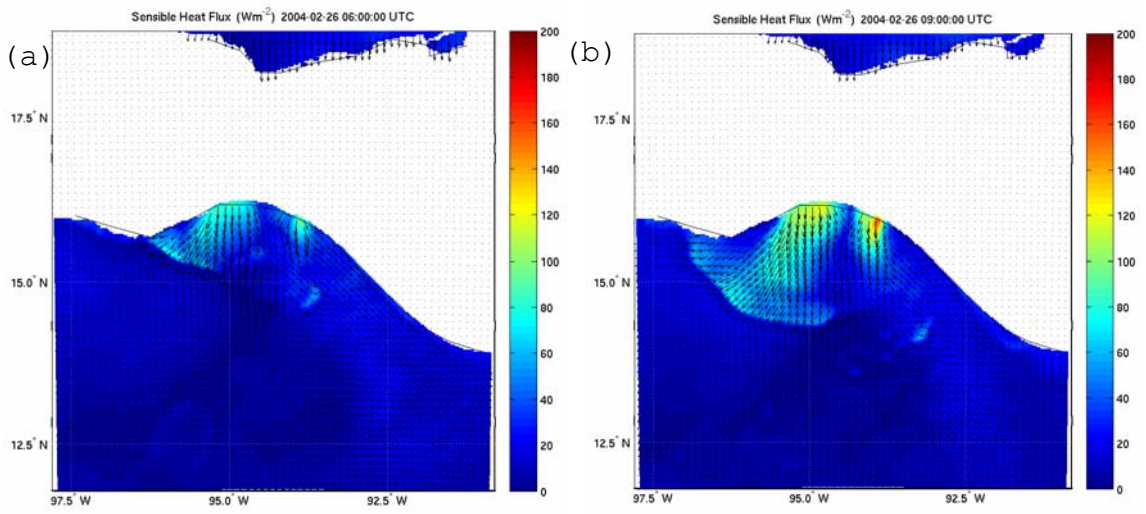

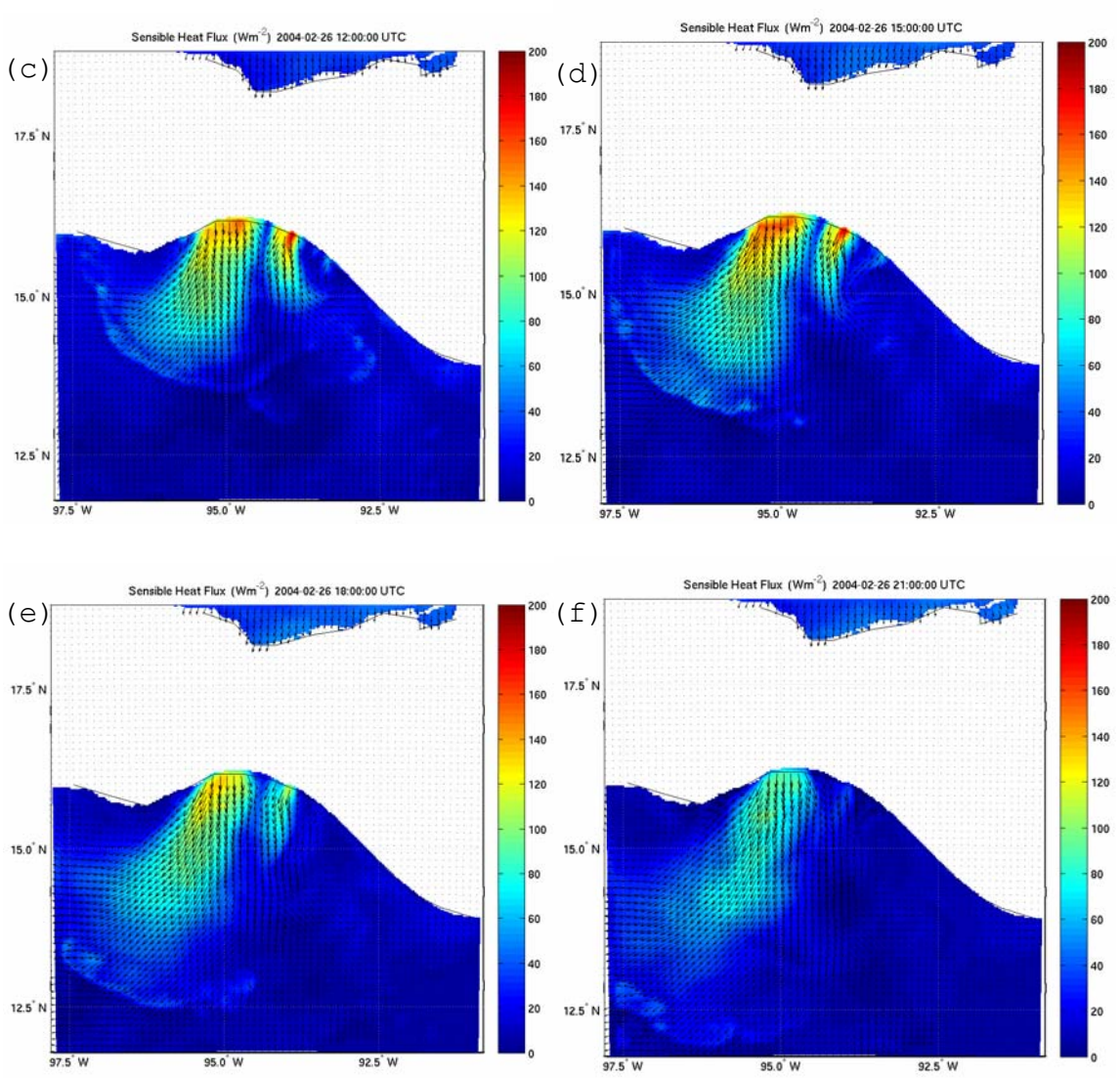

Figure 13. COAMPS simulated sensible heat flux contours in Wm^{-2} and wind vectors at 10 m analyzed on 26 February at (a) 06Z, (b) 09Z, (c) 12Z, (d) 15Z, (e) 18Z and (f) 21Z. The length of the wind vector is proportional to its magnitude.

The development of the latent heat flux on 26 February 2004 is shown in Figure 14. The maximum latent heat flux occurs when there is dry air combined with strong wind imparted on the warmer waters. There is also significantly larger latent heat flux to the atmosphere along the western boundary of the main outflow compared to the rest of the outflow. This feature coincides with the

drier air descending from higher terrain. Also, the secondary Chiapas outflow is drier and is seen to produce a much larger latent heat flux. Another feature of the latent heat flux is the apparent local maximum located where significant SST gradient as the flow moves over the sea.

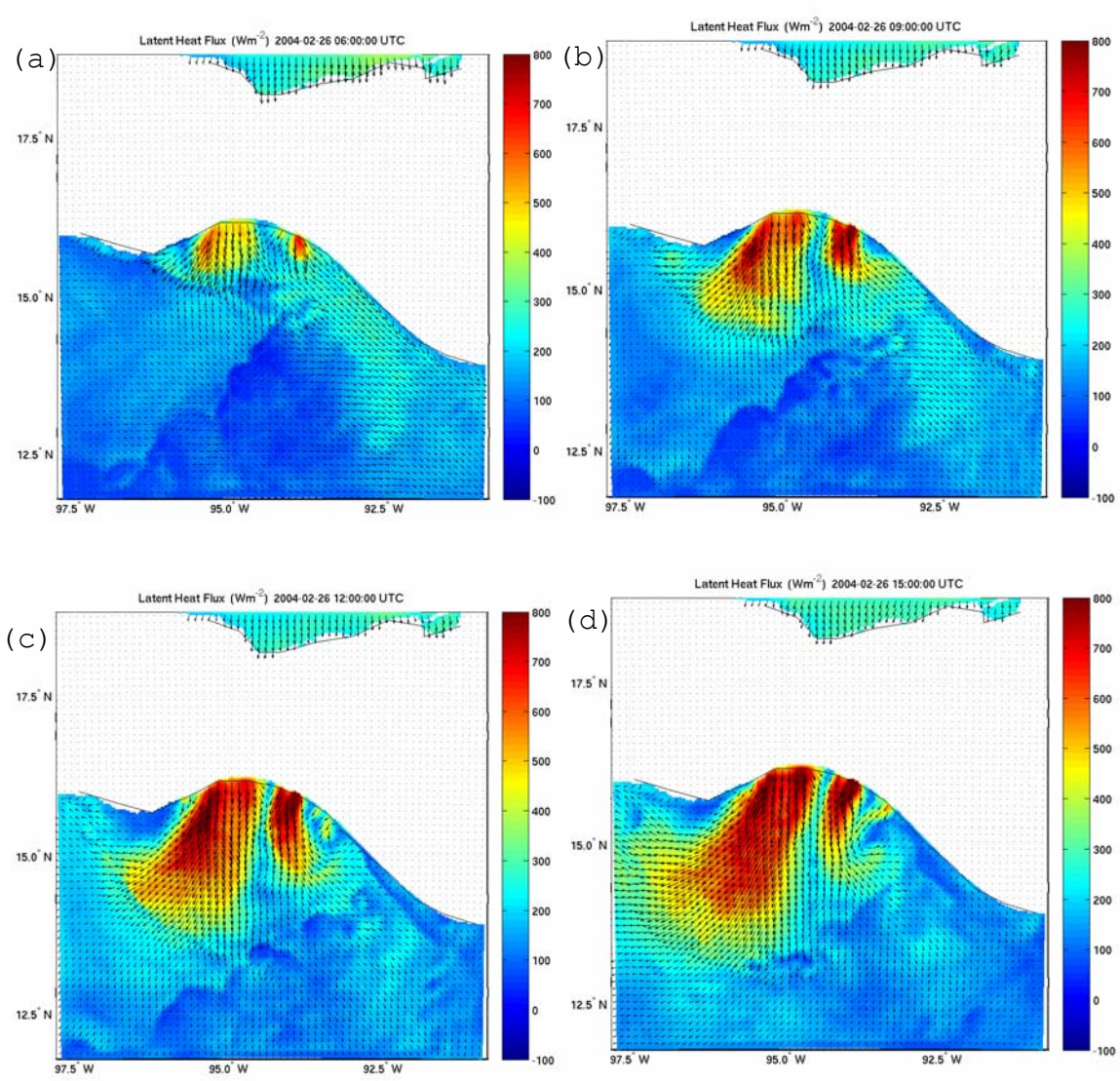

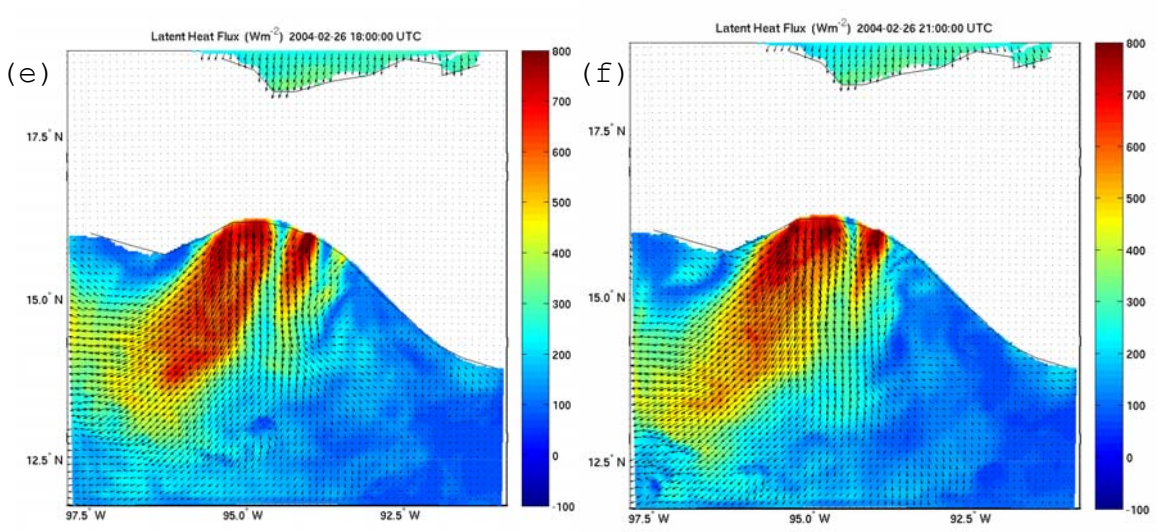

Figure 14. COAMPS simulated latent heat flux contours in Wm^{-2} and wind vectors at 10 m analyzed on 26 February at (a) 06Z, (b) 09Z, (c) 12Z, (d) 15Z, (e) 18Z and (f) 21Z. The length of the wind vector is proportional to its magnitude.

C. OBSERVED UPPER OCEAN RESPONSE TO GAP022604

1. Satellite Depiction of the Sea Surface Temperature Evolution

The SST field from several sources of satellite remote sensing (GOES 10-12, MODIS/Tera, and MODIS/Aqua) is displayed in Figure 15 for the period between 12Z of February 25 to 15Z of February 27, 2004. The difference between the six SST panels shows the time evolution of the SST field over a period of 51 hours. Different satellites/sensors were used to obtain the time evolution of the SST field.

Figure 15a shows the SST field about 12 hours before the onset of GAP022604. The basic feature of the SST field is the cool strip oriented in the northwest-southeast direction as outlined by the blue oval. The coolest water is located at Lat: 14°N, Lon: 94.4°W at 25.3°C. Noticeably, the mouth of the GoT near Lat: 16.1°N, Lon: 95°W was relatively warm at about 28°C. Warm water of about 29°C is

observed in most of the GoT region, particularly along the coastline to the east and west of the cool strip. The SST image in Figure 15b corresponds to about 4 hours after the GAP022604 front moved over water. The SST field at this hour is very similar to that 16 hours previous (Figure 15a) except for some cooling further off the coast near 14N latitude.

Significant SST changes occurred between 04:45Z (Figure 15b) and 07:30Z (Figure 15c) accompany the onset of the Tehuano. Figure 15c shows further cooling along the previous cool strip (blue oval), although the orientation remains nearly the same. The largest change occurs near the mouth of the gulf where a new cool strip exits along the northeast-southwest direction (orange oval) with the north-most tip at Lat: 16.1^{o}N, Lon: 95^{o}W. SST at the mouth of the gulf decreased from 28^{o}C to 24.5^{o}C during the three-hour period. From the COAMPS simulation discussed earlier and the scatterometer measurements (Cherrett, 2006), the location of this new cool strip is collocated with the outflow jet. The cooling is hence a result of the strong atmospheric forcing of the Tehuano.

Figures 15c and 15d also show the presence of another cooling spot (cyan circle) that was developed after the onset of GAP022604, where the SST dropped from 28.5^{o}C in Figure 15b to 26.5^{o}C three hours later. This newly developed cool spot confirms the existence of the secondary gap outflow that appeared in COAMPS simulations (Cherrett 2006, also shown here in the previous section).

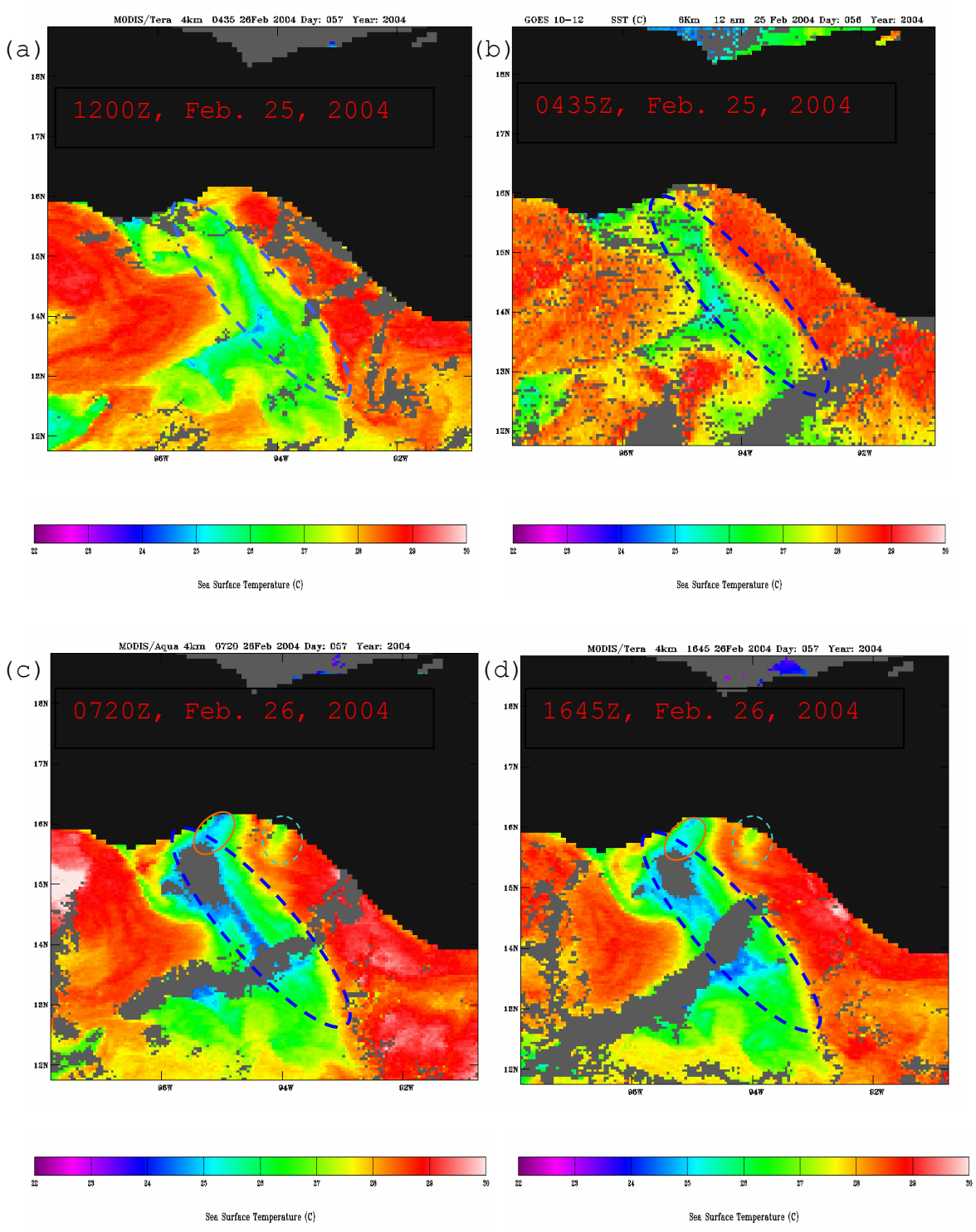
(a)
MODIS/Tera 4km 0435 26Feb 2004 Day: 057 Year: 2004
1200Z, Feb. 25, 2004
(b)
GOES 10-12 SST (C) 6Km 12 am 25 Feb 2004 Day: 056 Year: 2004
0435Z, Feb. 25, 2004
Sea Surface Temperature (C)
Sea Surface Temperature (C)
(c)
MODIS/Aqua 4km 0720 26Feb 2004 Day: 057 Year: 2004
0720Z, Feb. 26, 2004
(d)
MODIS/Tera 4km 1645 26Feb 2004 Day: 057 Year: 2004
1645Z, Feb. 26, 2004
Sea Surface Temperature (C)
Sea Surface Temperature (C)

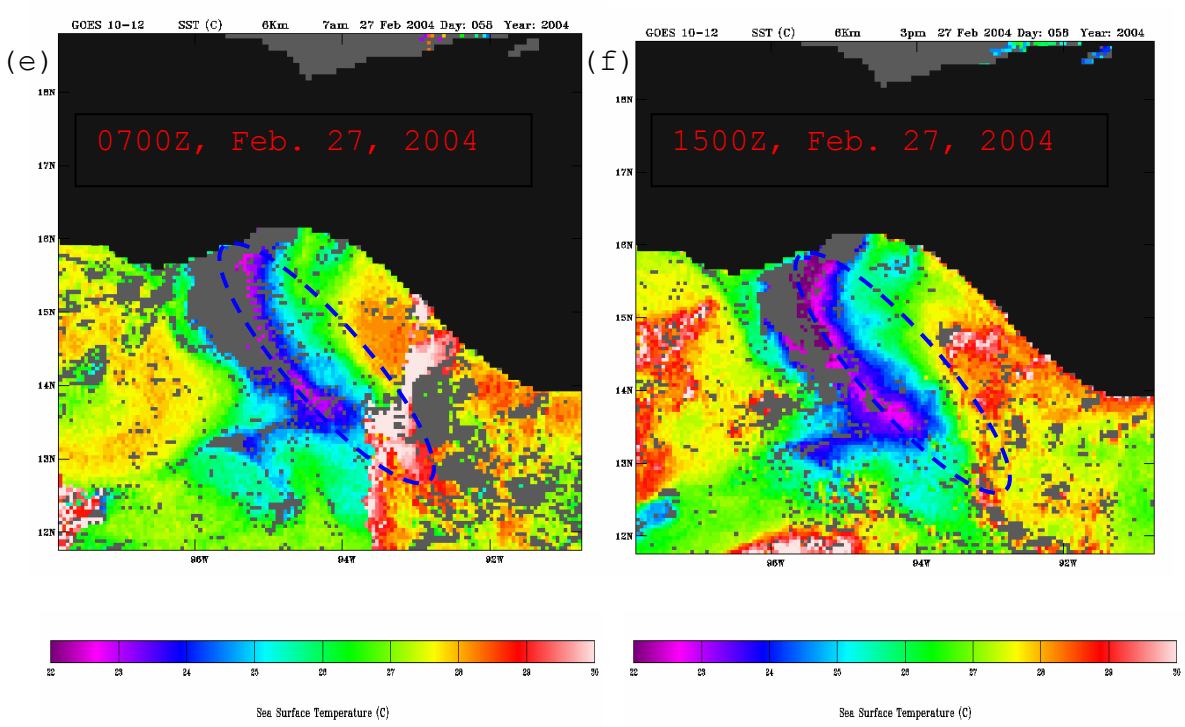

Figure 15. Sea surface temperature satellite images from GOES-12, MODIS/Aqua, MODIS/Terra on (a) 25 Feb. 12Z, (b) 26 Feb. 04:35Z, (c) 26 Feb. 07:20Z, (d) 26 Feb. 16:45Z, (e) 27 Feb. 07Z, and (f) 27 Feb. 15Z. The blue oval denotes the location of the cool strip on (a).

Figure 15d shows similar SST spatial variations as in Figure 15c with slight warming in the cool strips. Significant cooling occurs again from Figure 15d to 15e (07Z February 27, 2004) and continued to 15Z of February 27 (Figure 15f). It is seen in Figure 15e that the coolest spots in the north end of the blue oval cool strip appears to align with the orange cool strip at the mouth, which becomes more evident and extends further to the southwest direction eight hours later in Figure 15f. These developments suggest that the cooling was directly associated with the Tehuano event. As the nighttime continues from midnight (Figure 15e) to early morning

(Figure 15f), the entire region cools off and the blue cool strip appears to move towards the southwest direction.

In summary, the SST field from the satellite observations suggest the presence of a permanent cool strip along the northwest-southeast direction that also experience significant cooling in response to the Tehuano. The development of the cool strip near the coast also suggests the rapid response of the upper ocean in response to the Tehuano.

2. Aircraft Observed SST Field

Two research flights (RF09 and RF10) were made by the NCAR C-130 during the GAP022604 period. Flight nine (RF09) was flown on February 26, 2004, took off at about 14Z and landed at about 22Z. Flight ten (RF 10) took place on February 27, 2004 also from 14Z to 22Z.

Figure 16 shows the SST field from the C-130 when flying at a level below 50 m (to avoid significant effects of the atmosphere between the ocean surface and the onboard sensors). Since the COAMPS operational forecast for Central America (27 Km inner grid resolution) were used to help determine the presence of the gap outflow jet, most of the SST measurements shown in Figure 16 are from the 40 m straight legs that crossed the predicted jet axis. The SSTs from flights nine and ten show cool SSTs near the coast while higher temperatures were measured further offshore. Because the flight track orients in the northeast-southwest direction near the coast and beyond, the C130 measured the cool strip development after the onset of the Tehuano near the coast (orange oval). However, the flight could not capture the cool water along the northwest-southeast direction (blue oval).

(a)

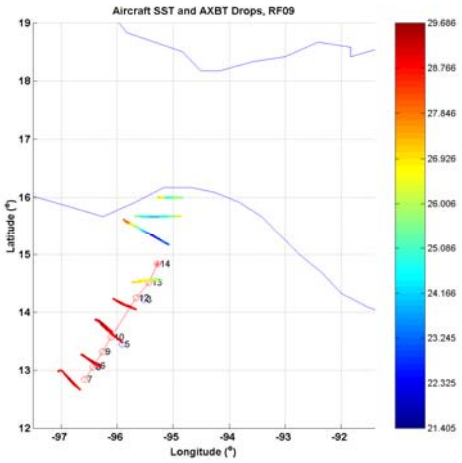

(b)

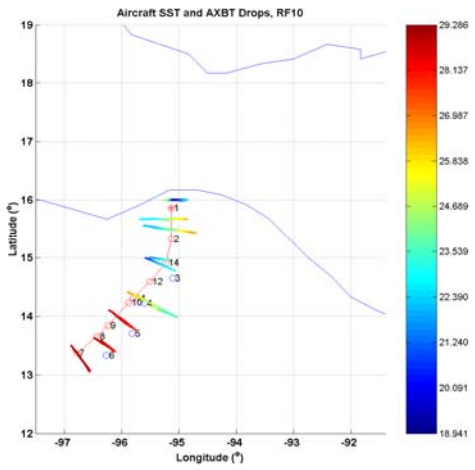

Figure 16. Flight tracks of NCAR C-130 and SST variation along the track. (a) RF09, (b) RF10. The circles with numbers denote the location of the AXBT drops.

3. Observed Thermocline Structure

During RF09 and RF10 of the NCAR C-130, AXBTs were dropped along the flight path (Figure 16). Most of the time, the flight path during the drop is along the COAMPS predicted jet axis. Measurements of the AXBTs result in vertical temperature profiles along the track of the AXBT drop and hence provide a spatial variation of the ocean mixed layer depth, thermocline structure, and surface temperature in limited areas. Meanwhile, SST measurements made from the C-130 were taken in low-level leg across the predicted jet axis. The combined SST and AXBT measurements gave us a very good picture of the mixed layer and thermocline structure along aircraft's path.

The path of the AXBT drop and the aircraft-observed SST variation are shown in Figure 16. Figure 17 shows the variation of the water temperature with depth and distance along each AXBT drop trajectory (red circles connected by

solid red line on each subplot). The horizontal axes in Figure 17 is the distance from the location of the AXBT drop that is closest to the shoreline (denoted as a '*' in the circle). Larger distance thus means further away from the coast.

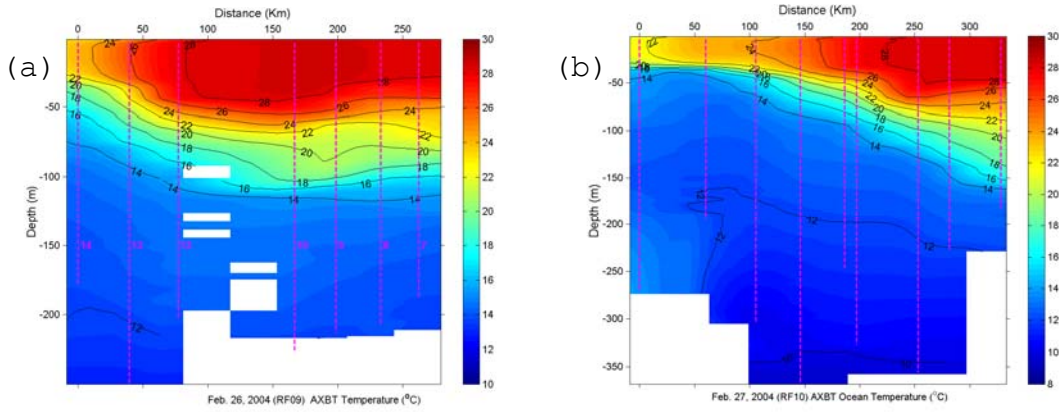

Figure 17. Vertical cross-section of water temperature from the AXBT measurements along the flight track. The corresponding flight track and the starting point ('*' in a red circle) are shown in Figure 16. The pink dash lines denote the location and depth of each AXBT drop that provide the data for these cross-section plots. The number in pink by each pink dash line denotes the AXBT drop number given in Figure 16 (a) from C-130 RF09; and (b) from C-130 RF10.

Figure 17a from RF09 shows that the SST was increasing from the starting point (AXBT #14) to further away from the coast. This trend of increasing SST continues up to a distance of 180 km (AXBT #10) where the maximum temperature (27.8°C) was found. The SST that corresponds to AXBT #14 (the starting location) was the lowest. Only a slight decrease of SST is observed further offshore until the end of the AXBT drop track (AXBT #7).

The mixed layer depth observed on February 26 2004 (RF09) followed almost the same pattern as the SST. The shallowest mixed layer of approximately 20 m was observed

at AXBT #14. At AXBT #10 (180 Km from AXBT #14) where the maximum SST occurred, the maximum mixed layer depth was found to be approximately 48 m. We find only a slight decrease of the mixed layer depth further away from coast.

Figure 17 also reveals the variation of the thermocline structure along the AXBT drop trajectory. We see the strongest thermocline strength (largest temperature gradient) near the coast while the vertical gradient relaxed beyond the location of AXBT #10 where the highest mixed layer temperature was found.

Figure 17b shows the vertical cross-section of water temperature on February 27 2004; almost one day after the onset of GAP022604. Locations of the AXBT drops during RF10 were different from those on the previous day. However, part of the RF10 drop trajectory (below 15^{o}N latitude) is close enough to RF09 to warrant a qualitative comparison. For purposes of comparison, a "new" cross section was created (Figure 18b) that uses the AXBT #14 of RF10 as the reference for distance calculation. Figure 18a is the same as Figure 17a for ease of comparison.

(a)

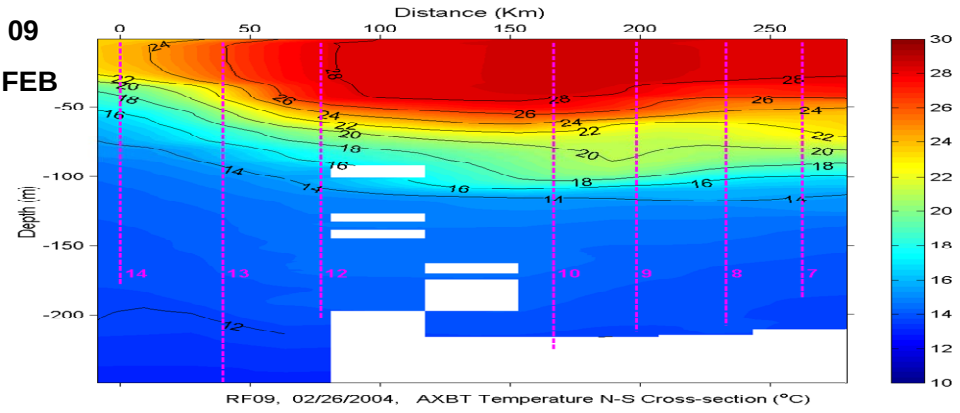

(b)

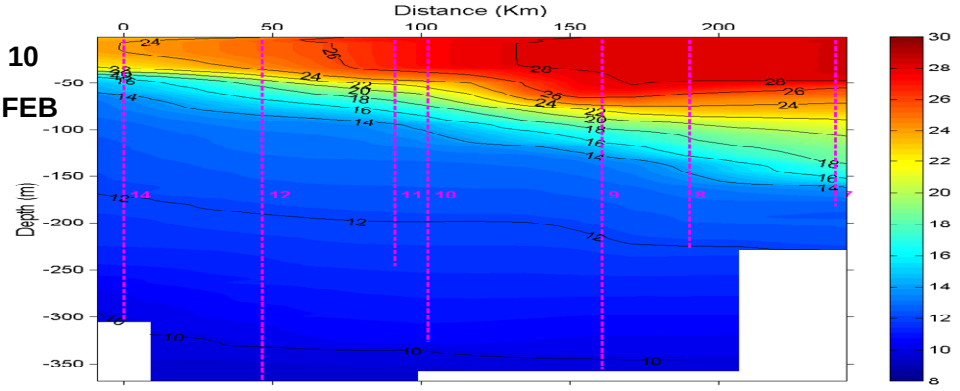

Figure 18. (a) same as Figure 17a; (b) portion of Figure 17b that is close to the location of the AXBT drop track in Figure 17a for RF09.

Figure 18b shows better defined ocean mixed layer in all AXBT measurements. The increasing SST moving along the aircraft's route from coast to open ocean is also observed. The depth of the mixing layer increases almost with the same pattern as the SST.

The sharpest thermocline gradient was observed near the coast and was reduced towards the open ocean. It is clear from Figure 18 that the thermocline was sharper than the previous day everywhere along the trajectory compared to that of the previous day. This indicates that the Tehuano event resulted in upwelling along the trajectory. Figure 18 also shows that the mixed layer temperature near

the coast was lower than the previous day by 2.7^{0}C, possibly caused by enhanced entrainment and cooling at the surface.

During GOTEX in 2004, a total of 88 AXBTs were deployed from 10 research flights. From these temperature profiles, a composite spatial distribution of mixed layer depth, mixed layer temperature, thermocline characteristics was made, and the mixed layer depth and temperature are shown in Figure 19. It should be noted that nearly all ten C-130 flights were made after the onset of Tehuano events. Figure 19 hence depicts a composite spatial variation when the mixed layer is or has been under the influence of a gap wind event. It should also be noted that the color filled contour of the variable is only meaningful wherever measurements are available (circles denote the location of a valid AXBT measurements that was used to generate the contour).

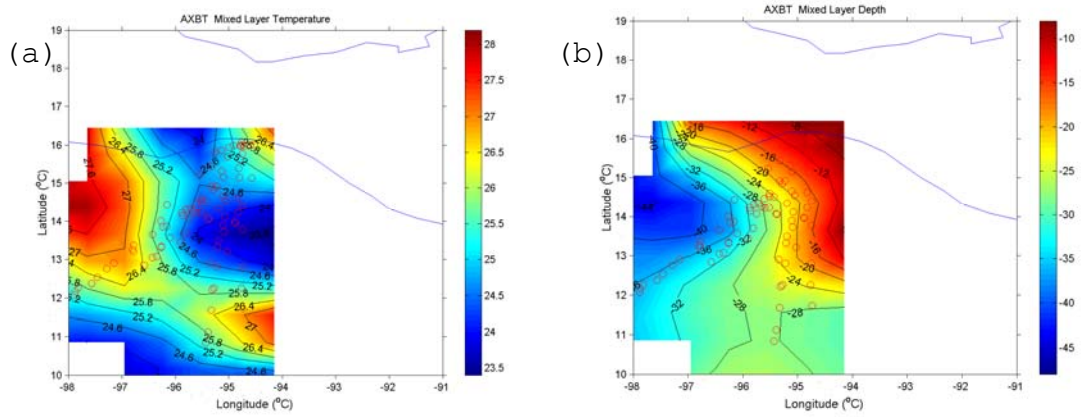

Figure 19. Composite mixed layer temperature from 88 AXBTs of the 10 C130 flights.

Figure 19 shows consistent deepening of the ocean mixed layer away from the mouth of the gulf. Near the gulf, the shallowest mixed layer is around 10 m in depth. The coolest water appears to be between 13^{o}N and 14^{o}N in

latitude and near 95°W longitude. These composites seem to depict a consistent spatial variation seen from the AXBTs of RF09 and RF10.

THIS PAGE INTENTIONALLY LEFT BLANK

V. MIXED LAYER SIMULATION OF THE UPPER OCEAN RESPONSE

A. OVERVIEW

The objective of the modeling effort of this thesis work is to understand the physical processes that dominante the observed SST and mixed layer temperature variation, both temporal and spatial, under strong atmospheric forcing. For this purpose, we prefer a model that is simple enough to allow us to isolate the different physical processes and flexible enough to be able to depict spatial variability. Running a mixed layer model on each COAMPS grid point with the corresponding forcing for the grid point seems to be an optimal solution.

The technical work involved in "coupling" COAMPS and the NPS Ocean Mixed Layer (OML) model is to use a "coupler" to read in COAMPS output on each grid, initiate the OML run for that grid, write the OML output for this particular grid, and move on to the next grid point. This "coupler", which we refer to as a "driver" is written as a UNIX script file. A MATLAB code was developed which transforms COAMPS output (flat files) in the right format in order to "feed" the OML model before the OML was called. Figure 20 shows the logical diagram of the model run process.

The COAMPS outputs that were used for OML model forcing include wind stress, latent heat flux, sensible heat flux, net solar irradiance, and net longwave gradient. Outputs from the OML includes the mixed layer depth, SST, salinity, and current velocity. Salinity effects were not considered in this modeling effort. Instead, salinity was set as a constant of 32 ppt.

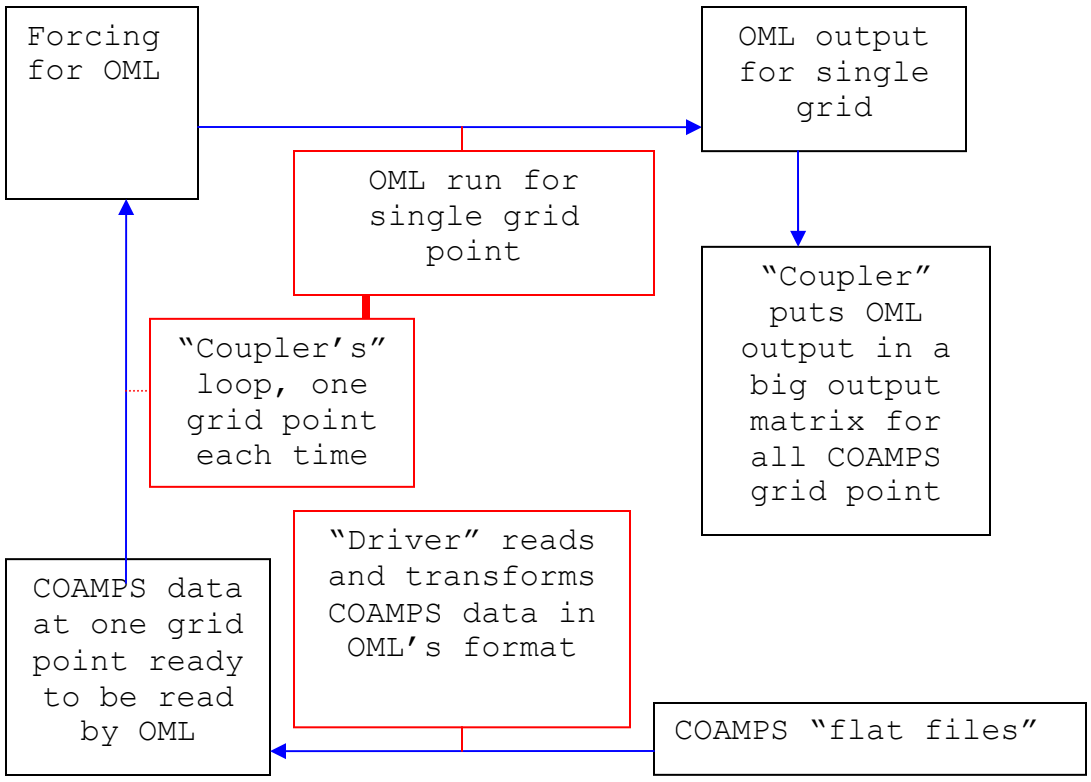

Figure 20. Logical diagram of forcing OML simulation process.

B. SIMULATIONS DESIGN, INITIAL THERMOCLINE CONDITIONS, AND ATMOSPHERIC FORCING

Ocean mixed layer simulations were designed to answer two fundamental questions of the upper ocean response to Tehuano.

1). In Tehuano events characterized by strong offshore wind, which physical process, mechanical mixing from the wind or thermally forced mixing/cooling from the surface heat flux, dominantes the changes in the upper ocean?

2). What are the roles of coastal and mesoscale upwelling and thermocline structure in determining the oceanic response to the gap events?

Table 1 lists the settings for eight OML simulations designed to answer these questions.

OML Simulation Settings				
NAME	TEMPERATURE PROFILE	UPWELLING	WIND STRESS	HEAT FLUXES
P2	AXBT 2, RF 10	NO	YES	YES
P2-H	AXBT 2, RF 10	NO	NO	YES
P2-S	AXBT 2, RF 10	NO	YES	NO
P2-W	AXBT 2, RF 10	YES	YES	YES
P8	AXBT 8, RF 10	NO	YES	YES
P8-H	AXBT 8, RF 10	NO	NO	YES
P8-S	AXBT 8, RF 10	NO	YES	NO
P8-W	AXBT 8, RF 10	YES	YES	YES

Table 1. List of model setting for each OML simulation.

In Table 1, the temperature profile refers to the vertical temperature profile that is used as the initial temperature at all levels from the surface down to 200 m. This profile not only sets the initial mixed layer temperature, but also and more importantly, sets up the thermocline depth and temperature gradient.

At the time of this thesis work, there were technical issues that prevented us from using different initial temperature profiles for each COAMPS grid point. As a result, a uniform initial and lower boundary (thermocline) condition was used for all grid points. This is obviously

unrealistic due to the strong variability of the upper ocean near the coast (see Figure 19). To evaluate the potential impact of this simplification, we chose two distinctively different temperature profiles as initial conditions. One of the profiles is taken from AXBT #2 in RF10, the other is from AXBT #8 in RF10 (see Figure 16 for locations). Simulations using the AXBT #2 profile closely resemble the near-coast regions, while those using AXBT #8 resemble the open ocean profiles. These profiles and the corresponding digitized profiles as OML model input are shown in Figure 21.

The first simulation in Table 1 (P2) uses the temperature profile of AXBT #2 with full COAMPS forcing from both surface stress and heat flux. This simulation is considered the "control run" which all other simulations will be compared with.

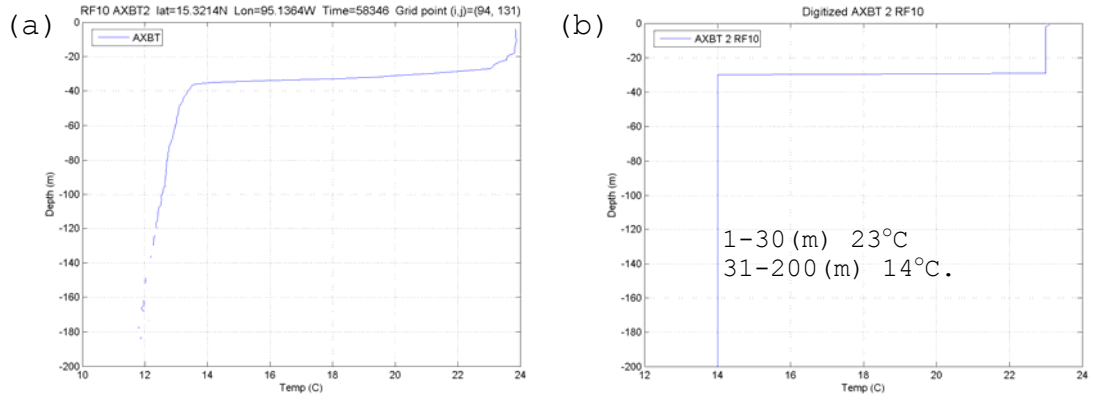

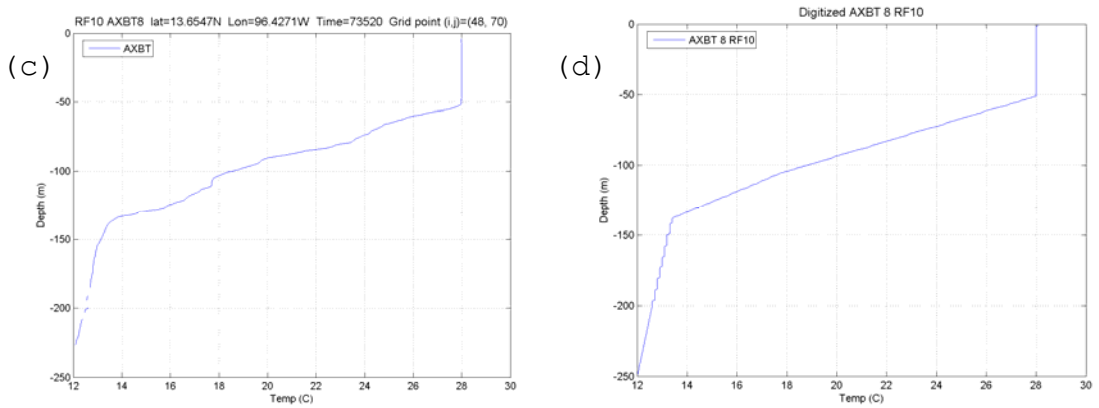

Figure 21. (a) and (c) temperature profiles from AXBTs #2 and #8 of RF10 respectively, (b) and (d) digitized profiles as input to the NPS OML.

Figure 22 shows an example of the COAMPS forcing at a near-coast location, Lat: 15.5°N, Lon: 95°W. The onset of GAP022604 at this location is clearly seen at 16 hours from 12Z of 25 February 2004, where surface stress increased from nearly zero to about 0.6 Nm^{-2}, 8 hours later at hour 24. During the same period, sensible heat flux increased from 0 to about 90 Wm^{-2} and latent heat flux increased from 120 to 650 Wm^{-2}. As a result, the net heat flux, the sum of sensible, latent, and IR heat fluxes, increased from 120 to 770 Wm^{-2}. The stress and heat flux decreased at hour 60 (00Z of February 28, 2004) although all variables are still higher than those prior to the onset of the high wind condition.

It is also noted that the sensible and latent heat fluxes both went through slight diurnal variation during GAP022604. This is consistent with the diurnal variation of air temperature (Figure 23). On the contrast, COAMPS SST remains constant within each 12 hour period, although it shows cooling at hour 36.

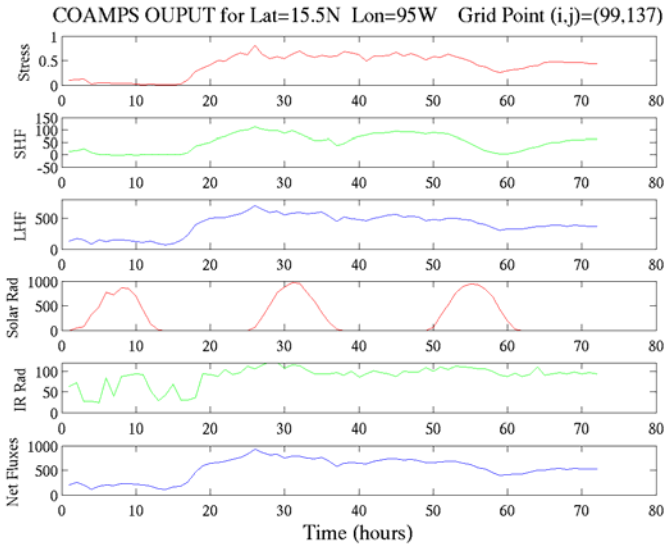

Figure 22. An example of the COAMPS forcing for the OML. From top to bottom, the panels show the surface wind stress (in Nm^{-2}), sensible heat flux (SHF, in Wm^{-2}), latent heat flux (LHF, in Wm^{-2}), solar irradiance (Solar Rad. in Wm^{-2}), net longwave irradiance (IR Rad. in Wm^{-2}), and the net heat flux (net fluxes, in Wm^{-2}).

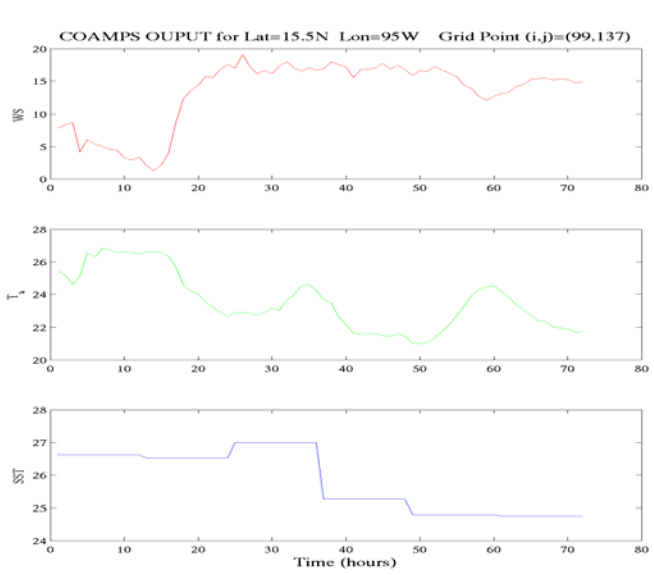

Figure 23. Same as in Figure 22, except for wind speed (top panel), air temperature (middle panel), and sea surface temperature (bottom panel).

For each simulation in Table 1, the OML run at each COAMPS grid point starts at 12Z of February 24, 2004 and continues for 96 hours. To avoid the effects of initial adjustment, analysis of the model results starts at 12Z of February 25, 2004. The time series plots to be shown in the next section will use day or hour as the horizontal axis with day 0 (hour 0) starting at 12Z of February 25, 2004.

C. MIXED LAYER MODEL RESULTS

1. Evolution of the Upper Ocean from the Control Simulation (P2)

In this section, we will examine the time evolution of the ocean mixed layer responding to forcing from the atmospheric Tehuano event using the results from the control simulation (simulation P2). Figure 24 shows the OML predicted change of SST at the onset of GAP022604 (Figure 24a,) and one, two days after (Figures 24b and 24c) based solely on the atmospheric forcing. Comparing to the COAMPS predicted surface momentum flux and net heat flux (Figure 22), it is not surprising to find cooling along the predicted jet axis even though the magnitude of cooling rate is smaller than the reported SST change in a Tehuano event (e.g., several degrees in hours, Stumpf 1975). The cooling continues where the maximum SST dropped by about 1^{o}C at 00Z of February 28. It is also noticed that the cooling in the vicinity of the jet axis is persistent throughout the Tehuano period, while the rest of the gulf region shows strong diurnal variation with warming during the day and cooling at night.

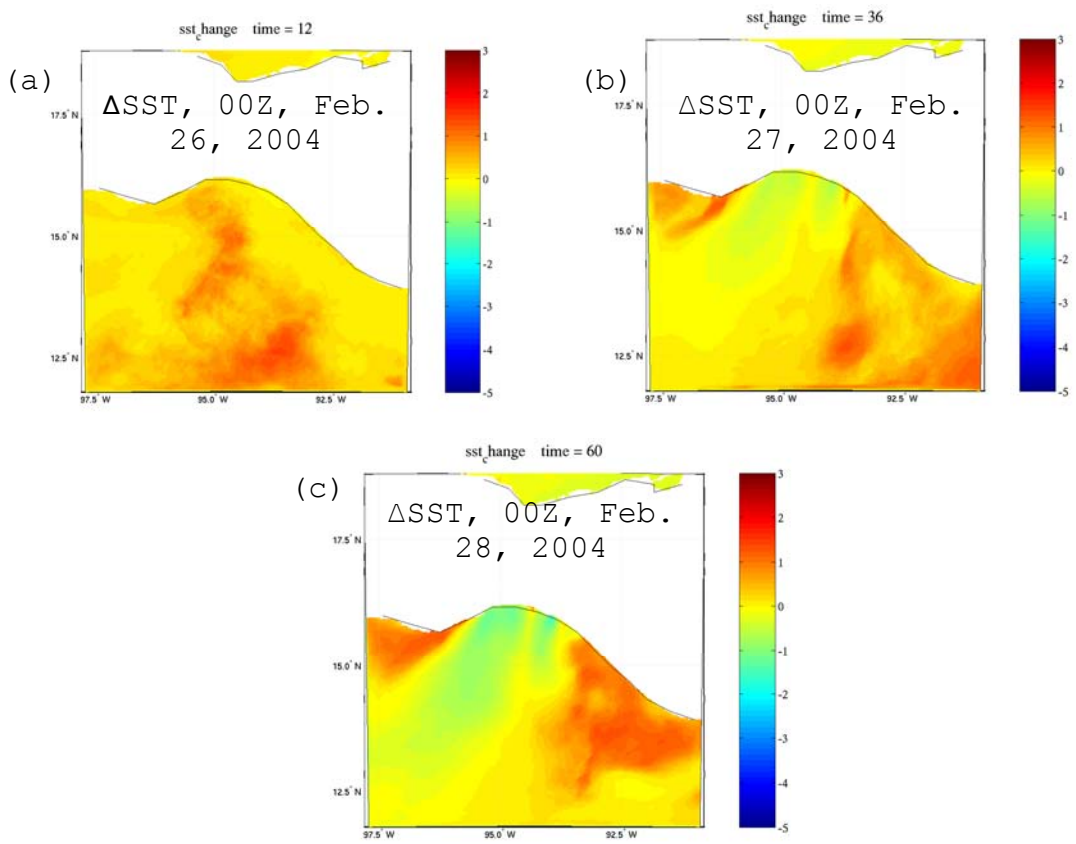

Figure 24. OML predicted change of SST at (a) 00Z, Feb. 26; (b) 00Z Feb. 27; and (c) 00Z Feb. 28 of 2004. The SST change refers to the difference in SSTs between the time shown and 12Z of February 25, 2004.

Figure 25a shows an example of the COAMPS SST field modified by the ΔSST from the OML (P2) simulation. The original COAMPS SST field and the satellite SST field are shown in Figures 25b and 25c for comparison. The difference between the original and the OML modified COAMPS SST field is mainly along the predicted jet axis, where the cooling of the upper ocean is explicitly resolved by the OML. Comparing with the satellite images, we find a similar SST pattern. The highest SSTs are displayed to the east and west of the jet axis and very near to the coast. The lowest temperatures are observed very close to the coast in the axis of the gap outflow. Hence, the modified SST field more

closely resembles more the satellite observation of the SST, particularly in the gulf region.

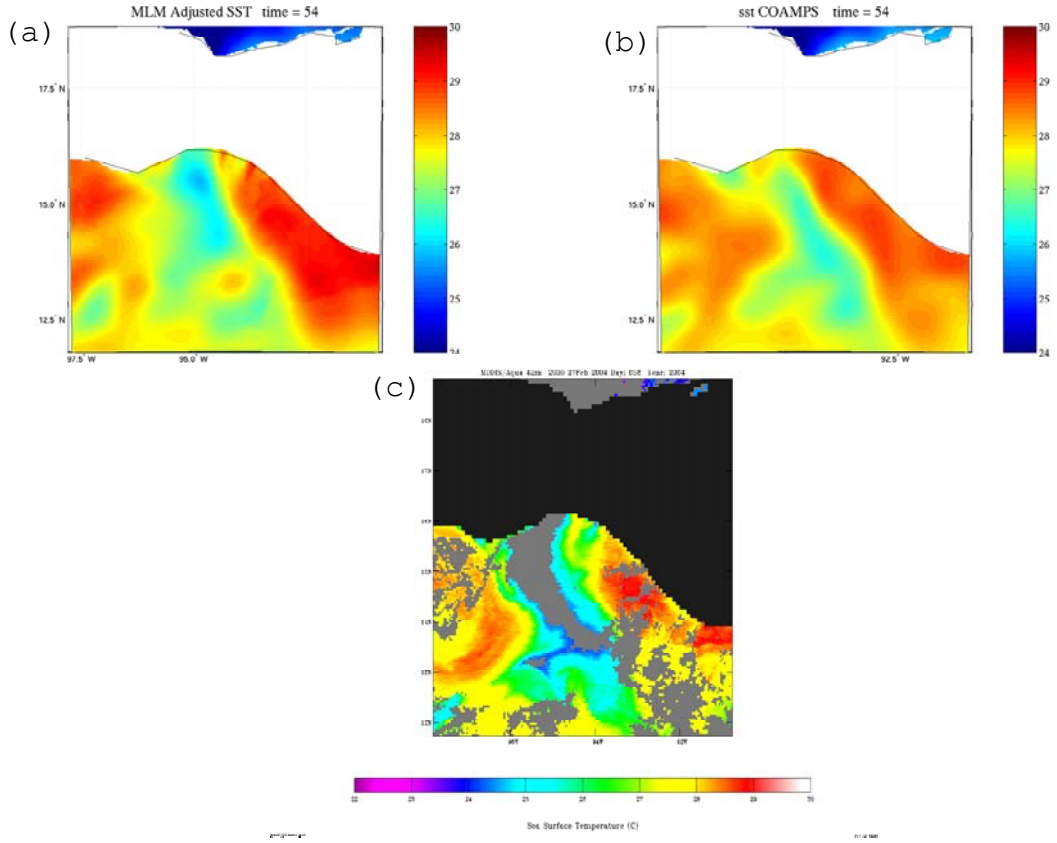

Figure 25. (a) OML adjusted COAMPS SST field on 1800 27 February 2004; (b) same as in (a), except for original COAMPS SST; (c) measurements of SST by MODIS/Aqua at 2030 27 February 2004.

Figure 26 shows the mixed layer depth contour plots with a 12-hour, interval from the "control run" (P2). The left panels show the daytime mixed layer depth (16:00 LST); while the right panels shows the early morning mixed layer depth (04:00 LST). Figure 26 shows that the daytime mixed layer is very shallow, below 10 m, everywhere except in the region of the gap outflow where the mixed layer depth is about 29 m. The deepest mixed layer is observed to be close

to the coast where the gap wind forcing is the strongest. During the night time to early morning period, the mixed layer deepens to around 29 m in most of the region, although the deepest mixed layer is still found along the predicted jet axis.

It is noted here that 29-30 m appear to be the limit of mixed layer deepening in this simulation. This is the result of the thermocline structure in the initial condition for this simulation (Figure 21b). The seasonal thermocline in P2 was set at 29 m below which a strongly stratified thermocline exists that limits the deeping of the upper mixed layer. In the next section, we will test the effect of the thermocline condition on the simulation.

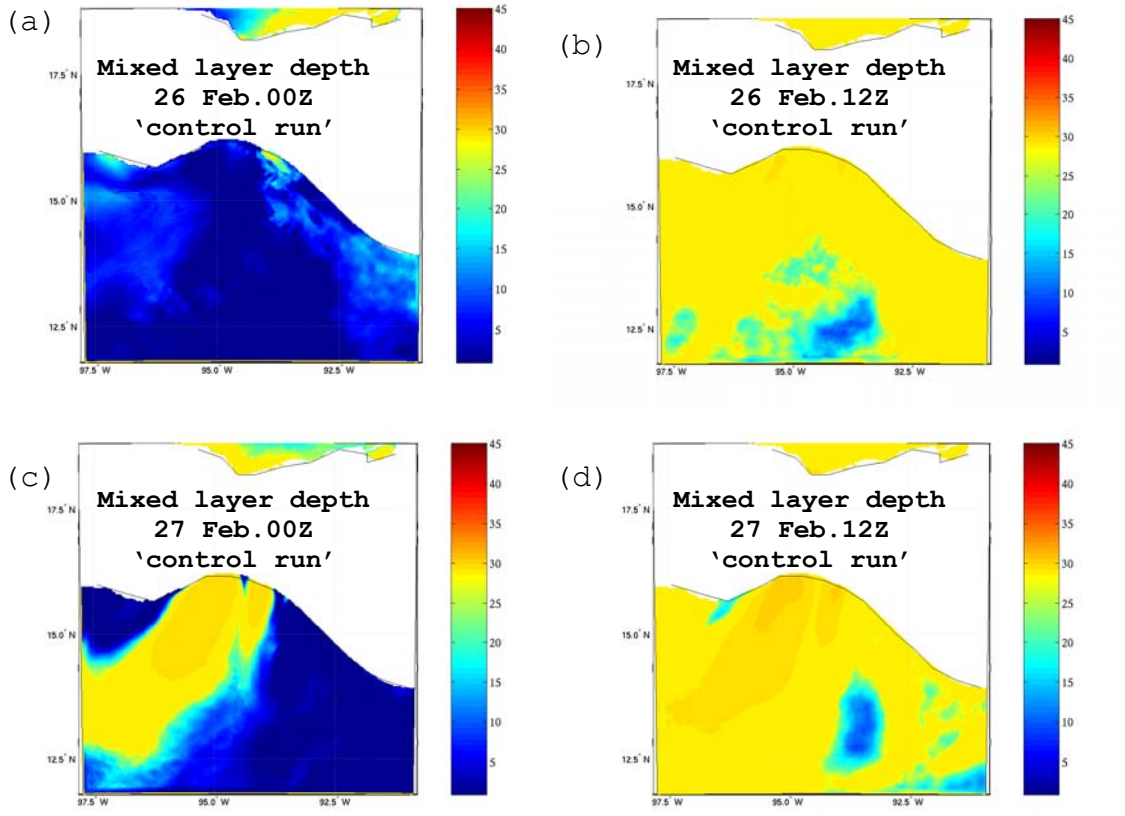

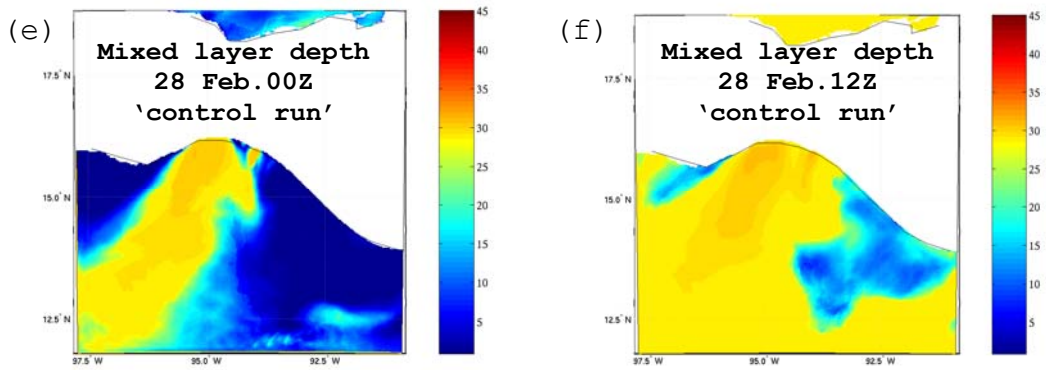

Figure 26. OML simulated mixed layer depth (m) for the control simulation (P2): (a) 00Z 26 Feb., (b) 12Z, 26 Feb., (c) 00Z 27, Feb., d) 12Z, 27 Feb. (e) 00Z 28 Feb., and (f) 12Z 28 Feb., 2004.

2. Physical Processes Controlling the Ocean Mixed Layer in GAP022604

a. Surface Stress vs. Net Heat Flux

It is seen in Figures 13, 14 that the gap event is accompanied by both enhanced surface wind stress and surface heat flux, and even the longwave irradiance (though not shown). In the region affected by the gap outflow, both surface stress (Figure 12) and surface net heat flux contribute to the enhanced turbulent mixing and cooling in the upper ocean. A comparison between simulations P2, P2H and P2S reveals the relative importance of each physical process (Figure. 27, 28 and 29).

Figures 27 shows the time variation of the OML predicted mixed layer depth (MLD), and the OML generated SST variation using the atmospheric forcing from the location of AXBT #2 in RF10 (Figure 16). The three simulations represent mixed layer forced by both stress and heat flux (P2), heat flux only (P2H), and surface stress only (P2S).

The COAMPS stress and net heat flux at the location of AXBT #2 show the arrival of GAP022604 at about 02Z of 26 February 2004 (0.6 day on the horizontal axis and 1800LST). Before the arrival of the gap outflow front, weak surface wind and negative net heat flux (the ocean is receiving heat from the atmosphere, presumably a result of solar radiation during the day), resulted in a shallow OML and the warmest SST for the next three days. During GAP022604, the time period where the net heat flux is negative is much shorter with smaller magnitude compared to the day before the gap event.

The P2S results are significantly different from those of P2 and P2H. With the stress only case (P2S), the mixed layer maintains its upper limit of 29-30 m (depth of the thermocline top) throughout the three-day simulation period. Results from P2 and P2H, on the other hand, are very similar in SST and MLD, except during the daytime of the third day, where shallowing of the mixed layer occurred in the heat flux only (P2H) simulation. This comparison suggests that the net heat flux is a dominant physical process that controls the mixed layer variation, especially the mixed layer temperature. This is a very interesting result as strong wind is considered the dominant phenomenon in a gap outflow event. Our result suggests that the enhanced heat flux loss of the upper ocean during the Tehuano largely controls the upper ocean properties.

Figure 28 shows similar results from an open ocean location (location of AXBT #8). Here, GAP022604 arrived at about 12Z 26 February, 2004 (04:00 LST), about 10 hours after it reached the location of AXBT #2. Mixed layer deepening at this location occurred long before the

arrival of the gap outflow front as a result of heat flux loss at the ocean surface after sunset. Cooling of the mixed layer only became significant after 1.5 days on the horizontal axis (00Z or 18 LST, 27 February), again after sunset.

For comparison purpose, the OML results at the east of the gap wind jet are shown in Figure 29. This location was not significantly affected by the gap event as evident from the variation of both stress and net heat flux. The similarity between the P2 and P2H simulation also revealed the dominant effects of the surface heat flux in determining the upper ocean properties.

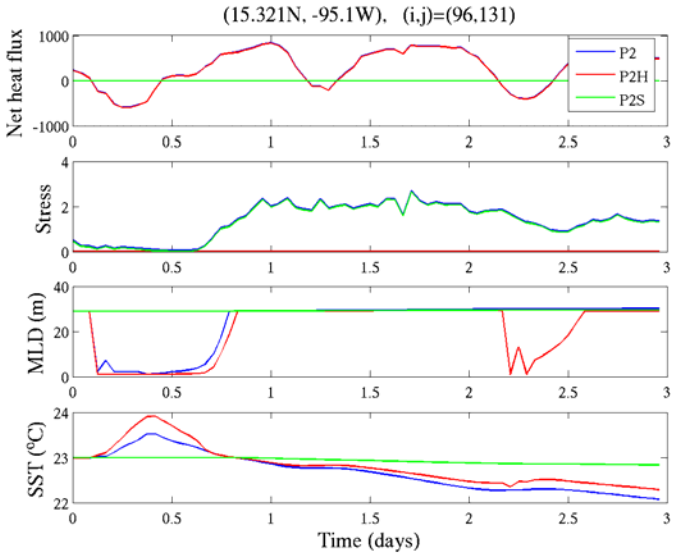

Figure 27. Comparison of atmospheric forcing, mixed layer depth, and SST from P2, P2H, and P2S simulations. The net heat flux is in Wm^{-2} and the stress is in Nm^{-2}. This time series is taken from the location of AXBT #2 in RF10 (Figure 16b). The horizontal axis denotes time (in day) from 1200Z 25 February 2004.

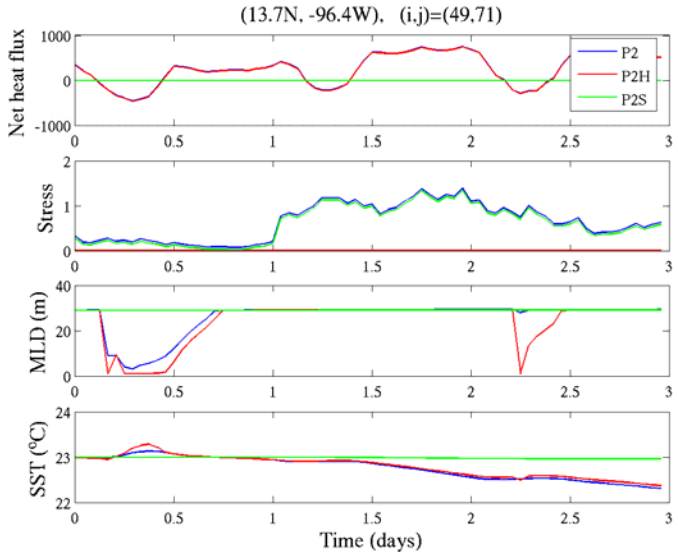

Figure 28. Same as Figure 27, except for an open ocean location (position of AXBT #8 in Figure 16).

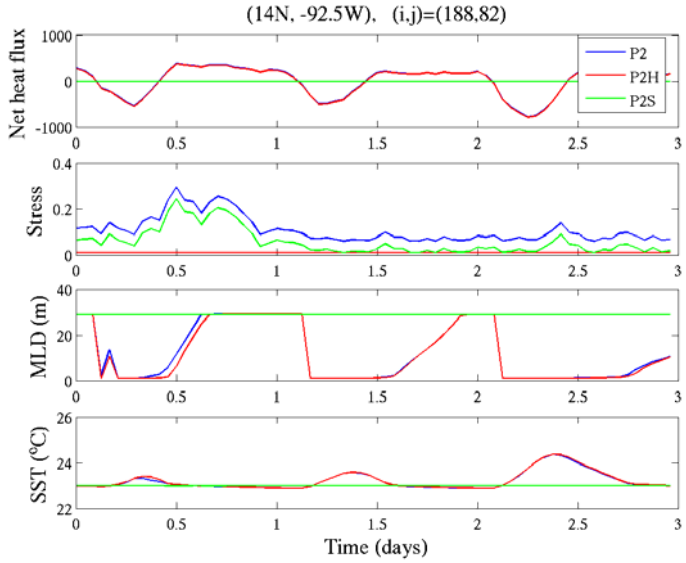

Figure 29. Same as in Figure 27, except for a location east of the gap outflow jet. Note the stress of P2 is elevated by 0.05 Nm^{-2} in order to differentiate the blue and the green lines).

b. Effects of Upwelling and Thermocline Structure

There are several limitations of the OML for applications involving spatial variability. These limitations include the effects of advection, the specified upwelling velocity, and the pre-determined thermocline structure. Although one can not easily correct these limitations, it is feasible to determine the effects of some of the limitations through sensitivity tests. In this section, we will analyze several model runs designed to examine the effects of upwelling and thermocline structure.

Figure 30 shows a comparison of both the effects of upwelling and the thermocline structure. Here, case P2 and P8 were simulated without upwelling effects, while the plots with '*' symbol are results from simulations with an upwelling velocity of 3 m day^{-1} added to the corresponding simulations (P2 or P8). The magnitude of the upwelling velocity is arbitrary but typical of coastal upwelling regions (Cushman-Roisin and O'Brien, 1983; Mc Creavy *et al.*, 1989; Kelley and Bourque, 1997). The value of 3 m day^{-1} was chosen simply to test sensitivity to a not-insignificant amount of vertical advection. The color of the plots are associated with different thermocline structure, where the blue lines are results from simulations using the AXBT #2 profile as the initial condition and the red lines are associated with the AXBT #8 temperature profile as the initial condition.

Figure 30 shows that the specification of upwelling velocity does not significantly affect the model results as the lines of the same color (with and without the '*' symbols) resemble each other rather closely. In

contrast, different thermocline structure results in significant change in both the MLD and the SST. With a shallow and strong thermocline (P2 and P2W), the mixed layer temperature is lower by 1 °C to 2 °C and with a stronger response to the gap wind forcing. Since the seasonal thermoclines typically have strong stable stratification, deepening of the mixed layer significantly below the thermocline is unlikely, as seen in Figure 31. Consequently, the depth of the top of the thermocline becomes a key factor in determining the upper ocean response to the strong gap wind forcing.

Figures 31 and 32 show similar inter-comparisons of the model results for an open ocean location (position of AXBT #8 in Figure 16) and the same location as that in Figure 30 where the gap outflow did not have a strong impact. These comparisons give the same conclusions as those from Figure 30.

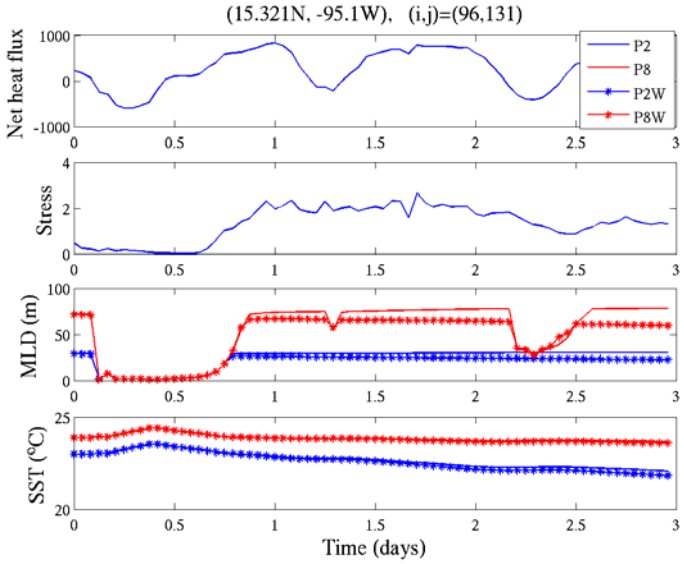

Figure 30. Time series plots for two "families" of runs, P2, P8

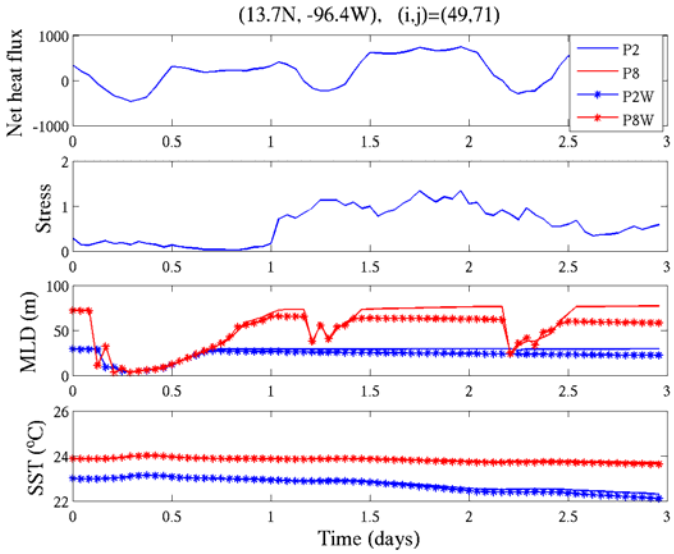

Figure 31. Same as in Figure 31 except at an open ocean location (position of AXBT #8).

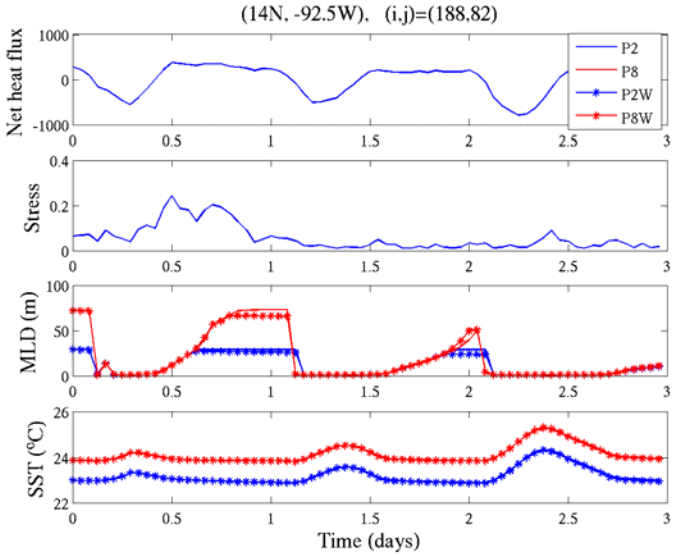

Figure 32. Same as in Figure 31, except at a location east of the gap outflow jet.

THIS PAGE INTENTIONALLY LEFT BLANK

VI. CONCLUSIONS AND DISCUSSIONS

This study focuses on understanding the development of the ocean response to gap outflow and the air-sea interaction processes during the 26^{th}-28^{th} February 2004 Tehuano event over the Gulf of Tehuantepec, Mexico. A high resolution mesoscale model, the U.S. Navy's Coupled Ocean Atmospheric Mesoscale Prediction System (COAMPS), was used to simulate the gap wind event and characterize the spatial and temporal variation of the momentum, sensible heat, and latent heat exchange at the ocean surface. These surface fluxes were used as the atmospheric forcing applied as the input to the NPS ocean mixed layer (OML) model.

The NPS OML model was used to simulate the oceanic response to the strong atmospheric forcing of the Tehuano. COAMPS forcing was used to drive the OML at every grid point of COAMPS inner-most domain. This process results in spatial and temporal variation of the mixed layer depth (MLD) and the SST.

SST measurements from satellites, coincident with in situ aircraft, and AXBTs collected during the Gulf of Tehuantepec Experiment (GOTEX), were used to evaluate and understand the COAMPS and OML model results. The AXBTs also provided vertical profiles of the ocean temperature from which the seasonal thermocline structure was obtained and used as input to the OML.

Simulation results from the mixed layer model suggest measurable SST evolution as a result of the enhanced upper ocean mixing along the jet axes within the time period when COAMPS SST was not updated. Comparisons with the SST field

from satellite images show the positive impact on the SST field when upper ocean mixing is considered in response to the gap out flow.

Our sensitivity tests show the dominant effects of surface heat flux (dominantly latent heat flux) in generating upper ocean mixing. In contrast, mechanical forcing by the strong wind of the gap outflow is not as important.

Sensitivity tests also suggest that the thermocline structure is the most important factor in determining the magnitude of the ocean response to the gap wind events. Variations in SST are not sensitive to upwelling for the time scale of less than three days.

The study of COAMPS/OML simulations and satellite (SST) images confirm the existence of a secondary gap outflow source in the area which exists at the south-east of the main gap outflow.

For future study, we suggest including variable, and hence more realistic, thermocline structure for different grid points while experimenting with “loose coupling”, i.e., perform COAMPS simulations using the OML modified SST field. The “loose coupling” approach will provide an assessment of the impact of the SST variation from the OML model run to the atmospheric model, which is an important step towards the development of a fully coupled atmospheric-ocean modeling system.

LIST OF REFERENCES

Adamec, D. and R. Elsberry, 1984: Sensitivity of mixed layer predictions at ocean station Papa to atmospheric forcing parameters. *J. Physical Oceanography.,* ***V14,*** *769-780.*

Cherrett, R. C., 2006: Observed and simulated temporal and spatial variations of gap outflow region. *NPS Thesis.*

Chu, P. C. and R. W. Garwood, Jr. 1990: The thermodynamic feedback between clouds and the ocean mixed layer. *Advances in Atmospheric Sciences.,* ***V7****, 1, 1-10.*

Clarke, A. J., 1988: Inertial wind path and sea surface temperature patterns near the Gulf of Tehuantepec and the Gulf of Papagayo. *J. Geophys. Res.*, **V93**, 15,491-15,501.

Gill, E. A., Atmospheric-Ocean Dynamics, 1982.Publisher.

Davidson, K. L. and R. W. Garwood, 1984: Coupled oceanic and atmospheric mixed layer model. *Dynam. of the Atm. and Oc.*, **V8**, 283-296.

Elsberry, L. R. and R. W. Garwood, 1980: Numerical ocean predictions models-Goal for the 1980s.*Bul. Amer. Soc.*, **61**, 12.

Garwood, W. R., 1977: An oceanic mixed layer model capable of simulating cyclic states. *J. Physical.Oceanography,* 7, 458-468.

Haack, T., S. Burck, C. Dorman, and D. Rogers, 2001: Supercritical Flow Interaction within the Cape Blanco-Cape Mendocino Orographic Complex. *Mon. Wea. Rev.*, **129**, 688-708.

Hodur, R. M., 1997: The Naval Research Laboratory's Couple Ocean/Atmosphere Mesoscale Prediction System (COAMPS), *Mon. Wea. Rev.*, **125**, 1414-1430.

Legeckis, R., 1988: Uppwelling off the Gulfs of Panama and Papagayo in the Tropical Pacific during March 1985, *J. Geoph. Res.*, **93**, C12, 15, 485-15, 489.

Liu, Q., C. Simmer and E. Ruprecht, 1997: Estimating Longwave Net Radiation at Sea Surface from the Special Sensor Microwave/Imager (SSM/I), ***J. Applied Meteo.***, **36**, 919-930.

Mass, C. F., S. Businger, M. D. Albright, and Z. A. Tucker, 1995: A windstorm in the lee of a gap in a coastal mountain barrier. ***Mon. Wea. Rev.***, **123**, 315-331.

Mc Creavy, J. P., H. S. Lee, and D. B. Enfield, 1989: The response to strong offshore winds: with applications to the Gulfs of Tehuantepec and Papagayo. J. Marine. Res., 47, 81-109.

NRL Publication, 2003:COAMPS model description general theory and equations, NRL/PU/7500—03-448.

Steenburgh, W. J., D. M Schumtz, and B. A. Colle, B., 1998: The Structure and Evolution of Gap Outflow over the Gulf of Tehuantepec. ***Mon. Wea. Rev.***, **126**, 2673-2690.

Sun, F. and J. Yu, 2006: Impacts of Central America gap winds on the SST annual cycle in the eastern Pacific warm pool. ***Geoph. Res. Let.***, **33**, L06710.

Xie, S., H. Xu, S. W. Kessler and M. Nonaka, 2005: Air–Sea Interaction over the Eastern Pacific Warm Pool: Gap Winds, Thermocline Dome, and Atmospheric Convection. ***J. Clim.***, **18**, 1.

INITIAL DISTRIBUTION LIST

1. Defense Technical Information Center
   Ft. Belvoir, Virginia

2. Dudley Knox Library
   Naval Postgraduate School
   Monterey, California

3. Chairman, Code 373
   Department of Meteorology
   Naval Postgraduate School
   Monterey, California

4. Professor Qing Wang, Code 373
   Department of Meteorology
   Naval Postgraduate School
   Monterey, California

5. Professor Roland W. Garwood, Code 372
   Department of Oceanography
   Naval Postgraduate School
   Monterey, California

6. Shouping Wang
   Naval Research Lab
   Monterey, California

7. LT Nikolaos Konstantinou H.N.
   Hellenic Navy General Staff
   Athens, Greece